

CAUSALLY ALIGNED CURRICULUM LEARNING

Mingxuan Li and Junzhe Zhang and Elias Bareinboim

Causal Artificial Intelligence Lab

Columbia University, USA

{ml, junzhez, eb}@cs.columbia.edu

ABSTRACT

A pervasive challenge in Reinforcement Learning (RL) is the “curse of dimensionality” which is the exponential growth in the state-action space when optimizing a high-dimensional target task (Bellman, 95). The framework of *curriculum learning* trains the agent in a curriculum composed of a sequence of related and more manageable source tasks. The expectation is that when some optimal decision rules are shared across source tasks and the target task, the agent could more quickly pick up the necessary skills to behave optimally in the environment, thus accelerating the learning process. However, this critical assumption of invariant optimal decision rules does not necessarily hold in many practical applications, specifically when the underlying environment contains *unobserved confounders*. This paper studies the problem of curriculum RL through causal lenses. We derive a sufficient graphical condition characterizing causally aligned source tasks, i.e., the invariance of optimal decision rules holds. We further develop an efficient algorithm to generate a causally aligned curriculum, provided with qualitative causal knowledge of the target environment. Finally, we validate our proposed methodology through experiments in high-dimensional confounded environments.

1 INTRODUCTION

As Roma was not built in one day, learning to achieve a complex task (e.g., cooking, driving) directly can be challenging. Instead, the human learning process is scaffolded with incremental difficulty to support the acquisition of progressively advanced knowledge and skills. The idea of training with increasingly complex tasks, known as curriculum learning, has been applied in reinforcement learning when Selfridge et al. (1985) used a carefully curated sequence of tasks to train agents to solve a modified Cart Pole system. In recent years, there has been a growing interest in automatically generating curricula tailored to the agent’s current capabilities, which opens up a new venue called “Automatic Curriculum Learning” (Portelas et al. 2020). An automatic curriculum generator requires two components: an encoded task space and a task characterization function (Narvekar et al. 2020; Wang et al. 2020). Task space encoding is often a bijective function that maps a task to a low dimensional vector (Parker-Holder et al. 2022; Klink et al. 2022; Florensa et al. 2018; Jiang et al. 2021; Portelas et al. 2019; Wang et al. 2019; 2020; Cho et al. 2023; Huang et al. 2022a). A proper task space encoding lays the foundation of a reasonable task characterization function measuring the fitness of tasks (Florensa et al. 2018; Dennis et al. 2020; Andreas et al. 2017; Sukhbaatar et al. 2018; Jiang et al. 2021). New training tasks, called source tasks, are generated by changing the target task’s state space or parameters of transition functions in the encoded task space. A system designer then determines in which order the agent should be trained in these source tasks, following the task characterization function. The set of generated source tasks and the training order defined upon this set defines a *curriculum* for the learning agent. Please see App. G for more related work.

While impressive, most curriculum RL methods described so far rely on the assumption that generated source tasks are aligned with the target. Consequently, the agent could pick up some valuable skills by training in such source tasks, allowing it to behave optimally in certain situations in the target environment. However, this critical assumption does not necessarily hold in many real-world decision-making settings. For concreteness, consider a modified Sokoban game shown in Fig. 1 inspired by Schrader (2018) where an unobserved confounder U_t randomly determines the box color C_t (0 for yellow, 1 for blue) at every time step t . The agent receives a positive reward Y_t only

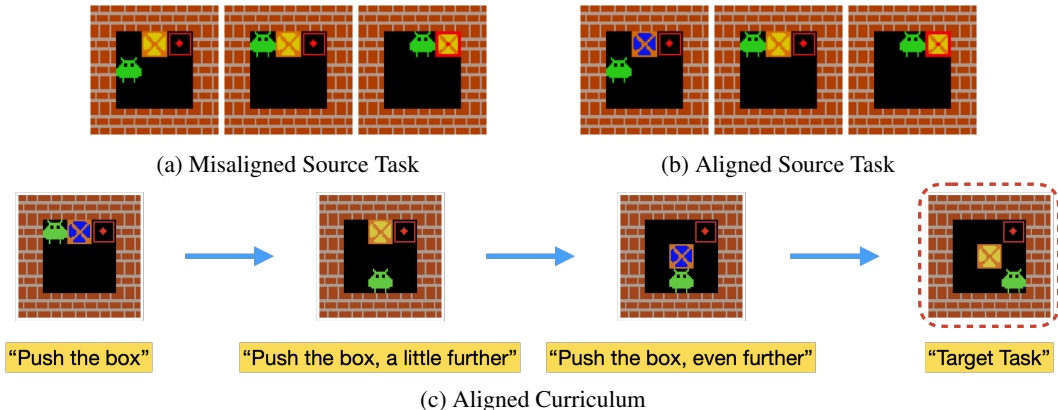


Figure 1: Examples of (a) full episode of a misaligned source task that intervenes in the box color, (b) full episode of an aligned source task that only changes the initial box location, and (c) an aligned curriculum where none of the source tasks intervenes in the box’s color.

when it pushes the box to the goal state when the box color appears yellow ($U_t = 0$); otherwise, it gets penalized ($U_t = 1$). We apply several state-of-the-art curriculum generators that construct source tasks by fixing the box color to yellow or blue, including ALP-GMM (Portelas et al., 2019), PLR (Jiang et al., 2021), Goal-GAN (Florensa et al., 2018), and Currot (Klink et al., 2022). Fig. 1a shows an example of the generated source tasks. We evaluate agents’ performance trained by those generated curricula and compare it with the one directly trained in the target task. Surprisingly, simulation results shown in Fig. 2 reveal that agents trained by the curricula failed to learn to push the yellow box to the destination. This suggests source tasks generated by intervening in the box color are misaligned; that is, training in these source tasks harms the agents’ target task performance.

Several observations follow from the Sokoban example. (1) A curriculum designer generates source tasks by modifying the data-generating mechanisms in the target tasks. (2) Such modifications could lead to a shift in system dynamics between the target task and source tasks. When this distribution shift is significant, training in source tasks may harm the agent’s learning. (3) The agent must avoid misaligned source tasks to achieve optimal learning performance. There exist methods attempting to address the challenges of misaligned source tasks leveraging a heuristic similarity measure between the target and source tasks (Svetlik et al., 2017; Silva & Costa 2018). Yet, a systematic and theoretically justified approach for exploiting other types of knowledge, e.g., qualitative, about the target task is missing.

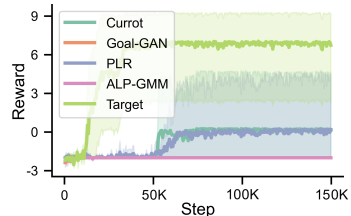


Figure 2: The average performance of curriculum generators.

This paper aims to address the challenges of misaligned source tasks in curriculum generation by exploring causal relationships among variables present in the underlying environment. To realize this, we formalize curriculum learning in the theoretical framework of structural causal models (SCMs) (Pearl, 2009). This formulation allows us to characterize misaligned source tasks by examining the structural invariance across the optimal policies obtained from the target and source tasks. More specifically, our contributions are summarized as follows. (1) We derive a sufficient graphical condition determining potentially misaligned source tasks. (2) We develop efficient algorithms for detecting misaligned source tasks and constructing source tasks that are guaranteed to align with the target task. (3) We introduce a novel augmentation procedure that enables state-of-the-art curriculum learning algorithms to generate aligned curricula to accelerate the agent’s learning. Finally, we validate the proposed framework through extensive experiments in various decision-making tasks.

1.1 PRELIMINARIES

This section introduces necessary notations and definitions that will be used throughout the discussion. We use capital letters (X) to denote a random variable, lowercase letters (x) to represent a

specific value of the random variable, and $\Omega(\cdot)$ to denote the domain of a random variable. We use bold capital letters (\mathbf{V}) to denote a set of random variables and use $|\mathbf{V}|$ to denote its cardinality.

The basic semantical framework of our analysis rests on *structural causal models* (SCMs) (Pearl, 2009; Bareinboim & Pearl, 2016). An SCM \mathcal{M} is a tuple $\langle \mathbf{U}, \mathbf{V}, \mathcal{F}, P \rangle$, where \mathbf{U} is a set of exogenous variables and \mathbf{V} is a set of endogenous variables. \mathcal{F} is a set of functions s.t. each $f_V \in \mathcal{F}$ decides values of an endogenous variable $V \in \mathbf{V}$ taking as argument a combination of other variables in the system. That is, $V \leftarrow f_V(\mathbf{PA}_V, \mathbf{U}_V)$, $\mathbf{PA}_V \subseteq \mathbf{V}$, $\mathbf{U}_V \subseteq \mathbf{U}$. Values of exogenous variables \mathbf{U} are drawn from the exogenous distribution $P(\mathbf{U})$. A policy π over a subset of variables $\mathbf{X} \subseteq \mathbf{V}$ is a sequence of decision rules $\{\pi(X|\mathbf{S}_X)\}_{X \in \mathbf{X}}$, where every $\pi(X|\mathbf{S}_X)$ is a probability distribution mapping from domains of a set of covariates $\mathbf{S}_X \subseteq \mathbf{V}$ to the domain of action X . An intervention following a policy π over variables \mathbf{X} , denoted by $\text{do}(\pi)$, is an operation which sets values of every $X \in \mathbf{X}$ to be decided by policy $X \sim \pi(X|\mathbf{S}_X)$ (Correa & Bareinboim, 2020), replacing the functions $f_{\mathbf{X}} = \{f_X : \forall X \in \mathbf{X}\}$ that would normally determine their values. For an SCM \mathcal{M} , let \mathcal{M}_π be a submodel of \mathcal{M} induced by intervention $\text{do}(\pi)$. For a set $\mathbf{Y} \subseteq \mathbf{V}$, the interventional distribution $P(\mathbf{Y}; \pi)$ is defined as the distribution over \mathbf{Y} in the submodel \mathcal{M}_π , i.e., $P_{\mathcal{M}}(\mathbf{Y}; \pi) \triangleq P_{\mathcal{M}_\pi}(\mathbf{Y})$; restriction \mathcal{M} is left implicit when it is obvious.

Each SCM \mathcal{M} is also associated with a causal diagram \mathcal{G} (e.g., Fig. 3a), which is a directed acyclic graph (DAG) where nodes represent endogenous variables \mathbf{V} and arrows represent the arguments $\mathbf{PA}_V, \mathbf{U}_V$ of each structural function $f_V \in \mathcal{F}$. Exogenous variables \mathbf{U} are often not explicitly shown by convention. However, a bi-directed arrow $V_i \leftrightarrow V_j$ indicates the presence of an unobserved confounder (UC), $U_{i,j} \in \mathbf{U}$ affecting V_i, V_j , simultaneously (Bareinboim et al., 2022). We will use standard graph-theoretic family abbreviations to represent graphical relationships, such as parents (*pa*), children (*ch*), descendants (*de*), and ancestors (*an*). For example, the set of parent nodes of \mathbf{X} in \mathcal{G} is denoted by $pa(\mathbf{X})_{\mathcal{G}} = \cup_{X \in \mathbf{X}} pa(X)_{\mathcal{G}}$. Capitalized versions *Pa, Ch, De, An* include the argument as well, e.g., $Pa(\mathbf{X})_{\mathcal{G}} = pa(\mathbf{X})_{\mathcal{G}} \cup \mathbf{X}$. A path from a node X to a node Y in \mathcal{G} is a sequence of edges that does not include a particular node more than once. Two sets of nodes \mathbf{X}, \mathbf{Y} are said to be d-separated by a third set \mathbf{Z} in a DAG \mathcal{G} , denoted by $(\mathbf{X} \perp\!\!\!\perp \mathbf{Y} | \mathbf{Z})_{\mathcal{G}}$, if every edge path from nodes in \mathbf{X} to nodes in \mathbf{Y} is “blocked” by nodes in \mathbf{Z} . The criterion of blockage follows (Pearl, 2009, Def. 1.2.3). For a more detailed survey on SCMs, we refer readers to (Pearl, 2009; Bareinboim et al., 2022).

2 CHALLENGES OF MISALIGNED SOURCE TASKS

This section will formalize the concept of aligned source tasks and provide an efficient algorithmic procedure to find such tasks based on causal knowledge about the data-generating process. Formally, a planning/policy learning task (for short, a task) is a decision-making problem composed of an environment and an agent. We focus on the sequential setting where the agent determines values of a sequence of actions $\mathbf{X} = \{X_1, \dots, X_H\}$ based on the input of observed states $\{\mathbf{S}_1, \dots, \mathbf{S}_H\}$. The mapping between states and actions defines the space of candidate policies, namely,

Definition 1 (Policy Space). For an SCM $\mathcal{M} = \langle \mathbf{U}, \mathbf{V}, \mathcal{F}, P \rangle$, a policy space Π is a set of policies π over actions $\mathbf{X} = \{X_1, \dots, X_H\}$. Each policy π is a sequence of decision rules $\{\pi_1(X_1|\mathbf{S}_1), \dots, \pi_H(X_H|\mathbf{S}_H)\}$ where for every $i = 1, \dots, H$,

- (i) Action X_i is a non-descendent of future actions X_{i+1}, \dots, X_H , i.e., $X_i \in \mathbf{V} \setminus De(\bar{\mathbf{X}}_{i+1:H})$;
- (ii) States \mathbf{S}_i are non-descendants of future actions X_i, \dots, X_H , i.e., $\mathbf{S}_i \subseteq \mathbf{V} \setminus De(\bar{\mathbf{X}}_{i:H})$.

Henceforth, we will consistently denote such a policy space by $\Pi = \{\langle X_1, \mathbf{S}_1 \rangle, \dots, \langle X_H, \mathbf{S}_H \rangle\}$.

The agent interacts with the environment by performing intervention $\text{do}(\pi), \forall \pi \in \Pi$ to optimize a reward function $\mathcal{R}(\mathbf{Y})$ taking a set of reward signals $\mathbf{Y} \subseteq \mathbf{V}$ as input.¹ A policy space, a reward function, and an SCM environment formalize a target decision-making task. We will graphically describe a target task using an augmented causal diagram \mathcal{G} constructed from the SCM \mathcal{M} ; actions \mathbf{X} are highlighted in blue; reward signals \mathbf{Y} are highlighted in red; input states \mathbf{S}_i for every action $X_i \in \mathbf{X}$ are shaded in light blue. For instance, Fig. 3a shows a causal diagram representing the

¹For instance, a cumulative discounted reward is defined as $\mathcal{R}(\mathbf{Y}) = \sum_{i=1}^H \gamma^{i-1} Y_i$ where $Y_i \in \mathbf{V}$, $i = 1, \dots, H$, are endogenous variables, and $\gamma \in (0, 1]$ is a discount factor.

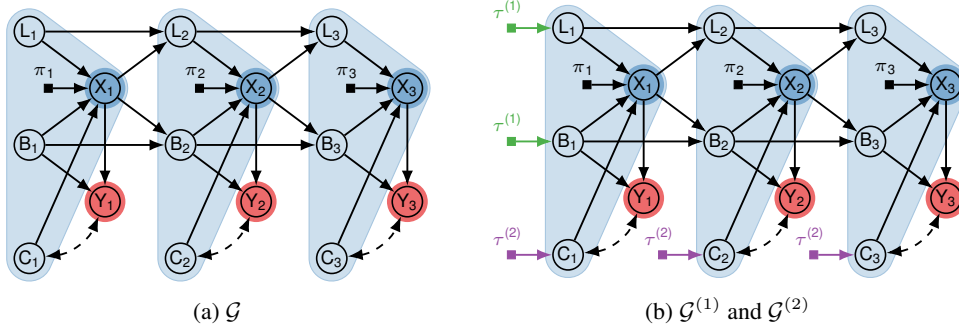


Figure 3: Causal diagram for (a) the target task \mathcal{T} ; and (b) comparing domain discrepancies between the target task \mathcal{T} and source tasks $\mathcal{T}^{(1)}$ and $\mathcal{T}^{(2)}$. (b) is (a) augmented by edit indicators.

decision-making task in the Sokoban game (Fig. 1). For every time step $i = 1, \dots, H$, L_i stands for the agent’s location, B_i for the box location, and C_i for the box color.

Definition 2 (Target Task). A target task is a tuple $\mathcal{T} = \langle \mathcal{M}, \Pi, \mathcal{R} \rangle$, where $\mathcal{M} = \langle \mathcal{U}, \mathcal{V}, \mathcal{F}, P \rangle$ is an SCM, Π is a policy space over actions $\mathbf{X} \subseteq \mathcal{V}$, and \mathcal{R} is a reward function over signals $\mathbf{Y} \subseteq \mathcal{V}$.

The goal is to find an optimal policy $\pi^* \in \Pi$ that maximizes the expected reward function $\mathbb{E}[\mathcal{R}(\mathbf{Y}); \pi]$ evaluated in the underlying environment \mathcal{M} , i.e.,

$$\pi^* = \arg \max_{\pi \in \Pi} \mathbb{E}_{\mathcal{M}} [\mathcal{R}(\mathbf{Y}); \pi]. \quad (1)$$

When the detailed parametrization of the SCM \mathcal{M} is provided, the optimal policy π^* is obtainable by applying planning algorithms, e.g., dynamic programming (Bellman, 1966) or influence diagrams (Koller & Milch, 2003). However, when underlying system dynamics are complex or the state-action domains are high-dimensional, it might be challenging to solve an optimal policy even with state-of-the-art planning algorithms. We will then consider the curriculum learning approach (Selfridge et al., 1985), where the agent is not immediately trained in the target task but provided with a sequence of related yet simplified source tasks.

Definition 3 (Source Task). For a target task $\mathcal{T} = \langle \mathcal{M}, \Pi, \mathcal{R} \rangle$, a source task $\mathcal{T}^{(j)}$ is a tuple $\langle \mathcal{M}^{(j)}, \Pi, \mathcal{R}, \Delta^{(j)} \rangle$ where $\mathcal{M}^{(j)}$ is an SCM compatible with the same causal diagram as \mathcal{M} , i.e., $\mathcal{G}_{\mathcal{M}} = \mathcal{G}_{\mathcal{M}^{(j)}}$; a set of variables $\Delta^{(j)} \subseteq \mathcal{V}$ is called *edits* where there might exist a discrepancy that $f_V \neq f_V^{(j)}$ or $P(U_V) \neq P^{(j)}(U_V)$ for every $V \in \Delta^{(j)}$.

In practice, source tasks are constructed from the target task by modifying parameters of the underlying structural functions \mathcal{F} or exogenous distributions $P(U)$. Consider again the Sokoban game described in Fig. 1. The system designer could generate a source task $\mathcal{T}^{(1)}$ by changing the agent and box’s initial location L_1, B_1 . Fig. 3b shows a causal diagram $\mathcal{G}^{(1)}$ representing the source task $\mathcal{T}^{(1)}$; $\tau^{(1)}$ is an *edit indicator* representing the domain discrepancies $\Delta^{(1)}$ between the target \mathcal{T} and source tasks $\mathcal{T}^{(1)}$. Here, arrows $\tau^{(1)} \rightarrow L_1, \tau^{(1)} \rightarrow B_1$ suggest that structural functions f_{L_1}, f_{B_1} or exogenous distributions $P(U_{L_1}, U_{B_1})$ have been changed in the source task $\mathcal{T}^{(1)}$ while other parts of the system remain the same as the target task \mathcal{T} .

By simplifying the system dynamics, learning an optimal policy in the source task $\mathcal{T}^{(j)}$ could be easier than in the target task \mathcal{T} . The expectation here is that the optimal decision rules $\pi^{(j)}$ over some actions $\mathbf{X}^{(j)} \subseteq \mathbf{X}$ remain invariant across the source and target tasks. If so, we will call such source tasks as *aligned*. Training in an aligned source task thus guides the agent to move toward an optimal policy π^* . For example, Fig. 1b shows an aligned source task for the Sokoban game where the agent and box’s locations are set close to the goal state. By training in the simplified task, the agent learns the optimal decision rule to push the yellow box to the goal state in this game.

²We will consistently use the superscript (j) to indicate a diagram $\mathcal{G}^{(j)} \triangleq \mathcal{G}_{\mathcal{M}^{(j)}}$ associated with a source task $\mathcal{T}^{(j)}$. Similarly, we write $P^{(j)}(\mathbf{Y}; \pi) = P_{\mathcal{M}^{(j)}}(\mathbf{Y}; \pi)$ and $\pi^{(j)} = \arg \max_{\pi \in \Pi} \mathbb{E}_{\mathcal{M}^{(j)}} [\mathcal{R}(\mathbf{Y}); \pi]$.

However, modifying the target task could lead to a misaligned source task whose system dynamics differ significantly from the target. Interestingly and more seriously, training in these source tasks may “harm” the agent’s performance, resulting in suboptimal decision rules, as illustrated next.

Example 1 (Misaligned Source Task). Consider the Sokoban game $\mathcal{T} = \langle \mathcal{M}, \Pi, \mathcal{R} \rangle$ described in Fig. 1. Fig. 3a shows its causal diagram \mathcal{G} . Specifically, the box color C_i (0 for yellow, 1 for blue) is determined by an unobserved confounder $U_i \in \{0, 1\}$ randomly drawn from a distribution $P(U_i = 1) = 3/4$. Box location B_i and agent location L_i are determined following system dynamics in deterministic grid worlds (Chevalier-Boisvert et al., 2018). The reward signal Y_i is given by,

$$Y_i = \begin{cases} 10 & \text{if } B_i = \text{“next to goal”} \wedge X_i = \text{“push”} \wedge (U_i = 0) \\ -10 & \text{if } B_i = \text{“next to goal”} \wedge X_i = \text{“push”} \wedge (U_i = 1) . \\ -0.1 & \text{otherwise} \end{cases} \quad (2)$$

If the agent pushes the box into the goal location (top right corner in Fig. 1), it receives a positive reward when the box appears yellow; it gets penalized when the box appears blue. Since $C_i \leftarrow U_i$, evaluating the conditional reward $\mathbb{E}[Y_i | b_i, c_i; \text{do}(x_i)]$ in the Sokoban environment \mathcal{M} gives,

$$\mathbb{E}[Y_i | B_i = \text{“next to goal”}, C_i; \text{do}(X_i = \text{“push”})] = \begin{cases} 10 & \text{if } C_i = 0 \\ -10 & \text{if } C_i = 1 \end{cases} \quad (3)$$

Thus, the agent should aim to push yellow boxes to the goal location in the target. The curriculum designer now attempts to generate a source task $\mathcal{T}^{(2)}$ by fixing the box color to yellow, i.e., $C_i \leftarrow 0$. Fig. 3b shows the causal diagram $\mathcal{G}^{(2)}$ associated with the source environment $\mathcal{M}^{(2)}$ where edit indicators $\tau^{(2)}$ denote the change in the structural function f_{C_i} determining the box color C_i . Evaluating the conditional reward $\mathbb{E}[Y_i | b_i; \text{do}(c_i, x_i)]$ in this manipulated environment $\mathcal{M}^{(2)}$ gives

$$\mathbb{E}^{(2)}[Y_i | B_i = \text{“next to goal”}; \text{do}(C_i = 0, X_i = \text{“push”})] = -5. \quad (4)$$

Detailed computations are provided in App. B. Perhaps counter-intuitively, pushing the yellow box to the goal location in the source task $\mathcal{T}^{(2)}$ results in a negative expected reward. This is because box color C_i is only a proxy to the unobserved U_i that controls the reward. Fixing C_i won’t affect Y but only breaks this synergy, hiding the critical information of U_i from the agent. Consequently, when training in the source task $\mathcal{T}^{(2)}$, the agent will learn to *never push* the box even when it is next to the goal location, which is suboptimal in the target Sokoban game \mathcal{T} . ■

2.1 CAUSALLY ALIGNED SOURCE TASK

Example 1 suggests that naively training in a misaligned source task may lead to suboptimal performance in the target task. The remainder of this section will introduce an efficient strategy to avoid misaligned source tasks, provided with the causal knowledge of the underlying data-generating mechanisms in the environment. For a target task $\mathcal{T} = \langle \mathcal{M}, \Pi, \mathcal{R} \rangle$, let \mathcal{G} be the causal diagram associated with \mathcal{M} . Let \mathcal{G}_π be an *intervened* diagram obtained from \mathcal{G} by replacing incoming arrows if action $X_i \in \mathbf{X}$ with arrows from input states \mathbf{S}_i for every action $X_i \in \mathbf{X}$. We first characterize a set of variables $\Delta^{(j)} \subseteq \mathbf{V}$ amenable to editing (for short, *editable states*) using independence relationships between edit indicators $\tau^{(j)}$ and reward signals \mathbf{Y} . Formally,

Definition 4 (Editable States). For a target task $\mathcal{T} = \langle \mathcal{M}, \Pi, \mathcal{R} \rangle$, let \mathcal{G} be a causal diagram of \mathcal{M} and $\mathbf{X}^{(j)} \subseteq \mathbf{X}$ be a subset of actions. A set of variables $\Delta^{(j)} \subseteq \mathbf{V} \setminus \mathbf{X}^{(j)}$ is *editable* w.r.t $\mathbf{X}^{(j)}$ if and only if $\forall X_i \in \mathbf{X}^{(j)}$, the following independence holds in the intervened diagram \mathcal{G}_π ,

$$\left(\tau^{(j)} \perp\!\!\!\perp \mathbf{Y} \cap \text{De}(X_i) \mid X_i, \mathbf{S}_i \right), \quad (5)$$

where $\tau^{(j)}$ is the set of added edit indicators pointing into nodes in $\Delta^{(j)}$.

For example, consider again the Sokoban game described in Example 1. The initial agent and box’s position $\Delta^{(1)} = \{B_1, L_1\}$ is editable with regard to all actions \mathbf{X} following Def. 4. Precisely, in the augmented diagram $\mathcal{G}^{(1)}$ of Fig. 3b, for every action $X_i \in \mathbf{X}$, the edit indicators $\tau^{(1)}$ are d-separated the reward signals $\mathbf{Y} \cap \text{De}(X_i) = \{Y_i, \dots, Y_H\}$ given input states $\{L_i, B_i, C_i\}$. On the other hand, the set of box color variables $\Delta^{(2)} = \{C_1, \dots, C_H\}$ are not editable w.r.t. actions \mathbf{X} since in the

augmented diagram $\mathcal{G}^{(2)}$ of Fig. 3b for every action $X_i \in \mathbf{X}$, there exists an active path between edit indicators $\tau^{(2)}$ and reward signals $\{Y_i, \dots, Y_H\}$ given action X_i and input states $\{L_i, B_i, C_i\}$, violating the criterion given by Def. 4

For a fixed policy $\pi \in \Pi$, for any subset $\mathbf{S} \subseteq \mathbf{V}$, we denote by $\Omega^{(j)}(\mathbf{S}; \pi) = \{\forall \mathbf{s} \in \Omega(\mathbf{S}) \mid P_{\mathcal{M}}(\mathbf{s}; \pi) > 0\}$ the set of *reachable* values of \mathbf{S} , which is the set of states that are possible to reach in a source task $\mathcal{T}^{(j)}$ under intervention $\text{do}(\pi)$. The following proposition establishes that modifying functions and distributions over a set of editable states $\Delta^{(j)}$ leads to an aligned source task.

Theorem 1 (Causally Aligned Source Task). *For a target task $\mathcal{T} = \langle \mathcal{M}, \Pi, \mathcal{R} \rangle$, let $\mathcal{T}^{(j)} = \langle \mathcal{M}^{(j)}, \Pi, \mathcal{R}, \Delta^{(j)} \rangle$ be a source task of \mathcal{T} by modifying states $\Delta^{(j)} \subseteq \mathbf{V}$. If $\Delta^{(j)}$ is editable w.r.t some actions $\mathbf{X}^{(j)} \subseteq \mathbf{X}$, then for every action $X_i \in \mathbf{X}^{(j)}$,*

$$\pi_i^*(X_i \mid \mathbf{s}_i) = \pi_i^{(j)}(X_i \mid \mathbf{s}_i), \quad \forall \mathbf{s}_i \in \Omega^{(j)}(\mathbf{S}_i; \pi^{(j)}) \cap \Omega(\mathbf{S}_i; \pi^*) \quad (6)$$

where $\pi^*, \pi^{(j)} \in \Pi$ are optimal policies in the target \mathcal{T} and source $\mathcal{T}^{(j)}$ tasks, respectively.

Thm. 1 implies that whenever states $\Delta^{(j)}$ is editable w.r.t. some actions $\mathbf{X}^{(j)}$, one could always construct an aligned source task $\mathcal{T}^{(j)}$ such that the optimal decision rules π^* over $\mathbf{X}^{(j)}$ is invariant across the target \mathcal{T} and source $\mathcal{T}^{(j)}$ tasks. Consequently, one could *transport* these optimal decision rules trained in the source task $\mathcal{T}^{(j)}$ without harming the agent’s performance in the target domain \mathcal{T} .³ For example, in the Sokoban game of Example 1, since initial states $\Delta^{(1)} = \{B_1, L_1\}$ is editable w.r.t. actions \mathbf{X} , moving the agent and box’s location leads to an aligned source task, which allows the agent to learn how to behave optimally when getting closer to the goal state. However, the performance guarantee in Thm. 1 does not necessarily hold when states $\Delta^{(j)}$ are not editable. For instance, recall that $\Delta^{(2)} = \{C_1, \dots, C_H\}$ are not editable in the Sokoban game. Modifying the box’s color could lead to a misaligned source task $\mathcal{T}^{(2)}$. An agent trained in this source task could pick up undesirable behaviors, as demonstrated in Example 1

Algo. 1 describes an algorithmic procedure, FINDMAXEDIT, to find a maximal editable set $\Delta^{(j)}$ in a causal diagram \mathcal{G} w.r.t. a set of actions $\mathbf{X}^{(j)} \subseteq \mathbf{X}$. A set of editable states $\Delta^{(j)}$ is maximal w.r.t. $\mathbf{X}^{(j)}$ if there is no other editable states $\Delta_*^{(j)}$ strictly containing $\Delta^{(j)}$. We always prefer a maximal editable set since it offers the maximum freedom to simplify the system dynamics in the target task. Particularly, FINDMAXEDIT iteratively adds endogenous variables $\mathbf{V} \setminus (\mathbf{X} \cup \mathbf{Y})$ to the editable states $\Delta^{(j)}$ and test the independence criterion in Def. 4. This procedure continues until it cannot add any more endogenous variables. Evidently, FINDMAXEDIT returns a maximal editable set $\Delta^{(j)}$ w.r.t. $\mathbf{X}^{(j)}$. A natural question arising at this point is whether the ordering of endogenous variables V changes the output. Fortunately, the next proposition shows that this is not the case.

Theorem 2. *For a target task $\mathcal{T} = \langle \mathcal{M}, \Pi, \mathcal{R} \rangle$, let \mathcal{G}_π be an intervened causal diagram of \mathcal{M} and let $\mathbf{X}^{(j)} \subseteq \mathbf{X}$ be a subset of actions. FINDMAXEDIT($\mathcal{G}_\pi, \mathbf{X}^{(j)}$) returns a maximal editable set $\Delta^{(j)}$ w.r.t actions $\mathbf{X}^{(j)}$; moreover, such a maximal set $\Delta^{(j)}$ is unique.*

Let n and m denote the number of nodes and edges in the intervened diagram \mathcal{G}_π and let d be the number of actions \mathbf{X} . Since testing d-separation has a time complexity of $\mathcal{O}(n + m)$, FINDMAXEDIT has a time complexity of $\mathcal{O}(d(n + m))$. We also provide other algorithmic procedures for directly deciding a set’s editability and constructing editable sets for a target task \mathcal{T} in App. C

³Causal aligned source tasks (Thm. 1) and editable states (Def. 4) are related to the concept of *transportability* in causal inference literature (Bareinboim & Pearl 2016), which generalizes estimation of unknown causal effects from different domains. Here we study the generalizability of an optimal decision policy.

3 CURRICULUM LEARNING VIA CAUSAL LENS

Once a collection of source tasks is constructed, the system designer could organize them into an ordered list, called a *curriculum*, as defined next:

Definition 5 (Curriculum). For a target task $\mathcal{T} = \langle \mathcal{M}, \Pi, \mathcal{R} \rangle$, a curriculum \mathcal{C} for \mathcal{T} is a sequence of source tasks $\{\mathcal{T}^{(j)}\}_{j=1}^N$, where $\mathcal{T}^{(j)} = \langle \mathcal{M}^{(j)}, \Pi, \mathcal{R}, \Delta^{(j)} \rangle$.

For instance, Fig. 1c describes a curriculum in the Sokoban game where the agent and the box are placed increasingly further away from the goal location. Given a curriculum \mathcal{C} , a typical curriculum learning algorithm trains the agent sequentially in each source task, following the curriculum’s ordering. Algo. 2 shows the pseudo-code describing this training process. It first initializes an arbitrary baseline policy $\pi^{(0)}$. For every source task $\mathcal{T}^{(j)} \in \mathcal{C}$, the algorithm updates the current

Algorithm 2: CURRICULUM LEARNING

Input: A curriculum \mathcal{C} .

Output: A policy $\pi^{(N)} \in \Pi$.

Initialize a baseline policy $\pi^{(0)}$;

for $j = 1, \dots, N$ **do**

Update a policy $\pi^{(j)}$ from $\pi^{(j-1)}$ such that

$$\pi^{(j)} = \arg \max_{\pi \in \Pi} \mathbb{E}_{\mathcal{M}^{(j)}} [\mathcal{R}(\mathbf{Y}); \pi] \quad (7)$$

return $\pi^{(N)}$;

policy $\pi^{(j-1)}$ such that the new policy $\pi^{(j)}$ is optimal in the source task $\mathcal{T}^{(j)}$. This step could be performed using a standard gradient-based algorithm, e.g., the policy gradient (Sutton & Barto 2018). The expectation is that, as the agent picks up more skills in the source tasks, it could consistently improve its performance in the target task or at least not regress.

Definition 6 (Causally Aligned Curriculum). For a target task $\mathcal{T} = \langle \mathcal{M}, \Pi, \mathcal{R} \rangle$, let $\mathcal{C} = \{\mathcal{T}^{(j)}\}_{j=1}^N$ be a curriculum for \mathcal{T} . Curriculum \mathcal{C} is said to be causally aligned with \mathcal{T} if for every $j = 1, \dots, N-1$, the set of invariant optimal decision rules across the source task and the target task expands, i.e.,

$$\left(\pi^{(j)} \cap \pi^* \right) \subseteq \left(\pi^{(j+1)} \cap \pi^* \right), \quad (8)$$

where $\pi^* \in \Pi$ is an optimal policy in the target task \mathcal{T} .

A naive approach to construct a causally aligned curriculum is to (1) construct a set of aligned source tasks by modifying editable states (Thm. 1) and (2) organize these tasks in an arbitrary ordering. However, the following example shows this is not a viable option.

Example 2 (Overwriting in Curriculum Learning). Consider a two-stage target task where action X_1 takes input H and X_2 takes input Z . The task SCM is, $H = U_H$, $Z = \neg X_1 \oplus U_Z$, $Y_1 = 0.5 * (H \oplus X_1)$, $Y_2 = \neg H \oplus X_2 \wedge Z$ where $P(U_Z = 1) = 1/2$, $P(U_H = 1) = 1/10$. Other than the reward Y_1, Y_2 , all other variables are binary. The optimal policy for the target task is $\pi^*(X_1 = \neg H|H) = 1$, $\pi^*(X_2 = 0|Z) = 1$. We create two source tasks. For $\mathcal{T}^{(1)}$, let $P(U_H = 1) = 9/10$ while other parts stay the same as target task \mathcal{T} . For $\mathcal{T}^{(2)}$, let $Z = \neg X_1$ while other parts stay the same as target task \mathcal{T} . From the causal diagram, we see that $\Delta^{(1)} = \{H\}$ is editable w.r.t $\mathbf{X}^{(1)} = \{X_1\}$ and $\Delta^{(2)} = \{Z\}$ is editable w.r.t $\mathbf{X}^{(2)} = \{X_2\}$.

Now if the agent is trained in a curriculum $\mathcal{C} = \{\mathcal{T}^{(1)}, \mathcal{T}^{(2)}\}$, its target task performance will deteriorate instead of improving. To witness, the optimal policy for X_2 in $\mathcal{T}^{(1)}$ is $\pi^{(1)}(X_2 = 1|Z) = 1$ and the optimal policy for X_1 in $\mathcal{T}^{(2)}$ is $\pi^{(2)}(X_1 = 0|H) = 1$. After training in $\mathcal{T}^{(1)}$, $\pi^{(1)}$ has an expected target task reward of 0.55 since $\pi^{(1)}(X_2 = 1|Z)$ is not optimal in the target yet. So, the agent proceeds to train in $\mathcal{T}^{(2)}$. It will learn the optimal target policy for X_2 , $\pi^*(X_2 = 0|Z) = 1$. But in the mean time, optimal policy of X_1 learned from $\mathcal{T}^{(1)}$, $\pi^*(X_1 = \neg H|H) = 1$, is also overwritten by $\pi^{(2)}$. The agent will only receive 0.5 in the target task, which is even worse than before training in $\mathcal{T}^{(2)}$. This suggests that curriculum \mathcal{C} is not causally aligned. ■

In the above example, the agent fails to learn an optimal policy due to “policy overwriting”. Fig. 4 provides a graphical representation of this phenomenon. Particularly, each source task $\mathcal{T}^{(1)}, \mathcal{T}^{(2)}$ covers one of the optimal decision rules over action X_1, X_2 , respectively. An agent trained in one of the source tasks, say $\mathcal{T}^{(1)}$, learns the optimal decision rule π_1^* for action X_1 , but forgets the

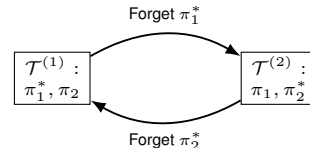


Figure 4: Policy overwriting described in Example 2

decision rule π_2^* for the other action X_2 learned previously in $\mathcal{T}^{(2)}$.

The same overwriting also occurs when the agent moves from task

$\mathcal{T}^{(2)}$ to $\mathcal{T}^{(1)}$. This means that regardless of how the system designer orders the curriculum, e.g., $\mathcal{C} = \{\mathcal{T}^{(1)}, \mathcal{T}^{(2)}, \mathcal{T}^{(1)}, \mathcal{T}^{(2)}, \dots\}$, the agent will always forget useful skills it picked up from previous source tasks, thus making it unable to achieve satisfactory performance in the target task. This example implies that there are more conditions for a curriculum to be ‘‘causally aligned’’.

3.1 DESIGNING CAUSALLY ALIGNED CURRICULUM

We will next introduce a novel algorithmic procedure to construct a causally aligned curriculum while avoiding the issue of overwriting. We will focus on a general class of *soluble* target tasks, which generalizes the *perfect recall* criterion (Koller & Friedman 2009) in the planning/decision-making literature (Lauritzen & Nilsson 2001).

Definition 7 (Soluble Target Task). A target task $\mathcal{T} = \langle \mathcal{M}, \Pi, \mathcal{R} \rangle$ is soluble if whenever $j < i$, $(Y \cap De(X_i) \perp\!\!\!\perp \pi_j | \mathcal{S}_i, X_i)$ in \mathcal{G}_π , where π_j is a newly added regime node pointing to X_j .

In words, Def. 7 says that for a soluble target task \mathcal{T} , for every action $X_i \in \mathbf{X}$, the input states \mathcal{S}_i summarizes all the states and actions’ history $\mathcal{S}_1, \dots, \mathcal{S}_{i-1}, X_1, \dots, X_{i-1}$. If this is the case, an optimal policy π^* for task \mathcal{T} is obtainable by solving a series of dynamic programs (Lauritzen & Nilsson 2001; Koller & Milch 2003). For instance, the Sokoban game \mathcal{T} graphically described in Fig. 3a is soluble. For every time step $i = 1, \dots, H$, given input states $\mathcal{S}_i = \{L_i, B_i, C_i\}$ and action X_i , regime variables π_1, \dots, π_{i-1} are d-separated from subsequent reward signals Y_i, \dots, Y_H .

Theorem 3 (Causally Aligned Curriculum). For a soluble target task $\mathcal{T} = \langle \mathcal{M}, \Pi, \mathcal{R} \rangle$, a curriculum $\mathcal{C} = \{\mathcal{T}^{(j)}\}_{j=1}^N$ is causally aligned if the following conditions hold,

- (i) Every source task $\mathcal{T}^{(j)} \in \mathcal{C}$ is causally aligned w.r.t. actions $\mathbf{X}^{(j)}$ (Def. 4);
- (ii) For every $j = 1, \dots, N - 1$, actions $\mathbf{X}^{(j)} \subseteq \mathbf{X}^{(j+1)}$.

Consider again the Sokoban game described in Fig. 3a. Let $\mathcal{C} = \{\mathcal{T}^{(j)}\}_{j=1}^H$ be a curriculum such that for every source task $\mathcal{T}^{(j)}$ is obtained by editing the agent and box’s location $\Delta^{(j)} = \{L_i, B_i\}$ at time step $i = H - j + 1$. We now examine conditions in Thm. 3 and see if \mathcal{C} is causally aligned. First, Condition (i) holds since every source task $\mathcal{T}^{(j)}$ is causally aligned w.r.t. actions $\mathbf{X}^{(j)} = \{X_{H-j+1}, \dots, X_H\}$ following discussion in the previous section. Also, Condition (ii) holds since for every $j = 1, \dots, H - 1$, actions $\mathbf{X}^{(j)} \subseteq \mathbf{X}^{(j+1)}$. This implies that one could construct a causally aligned curriculum in the Sokoban game by repeatedly editing the agent and box’ location following a reversed topological ordering; Fig. 1c describes such an example.

The idea in Thm. 3 suggests a natural procedure for constructing a causally aligned curriculum, which is implemented in FINDCAUSALCURRICULUM (Algo. 3). Particularly, it assumes access to a curriculum generator $\text{GEN}(\mathcal{T}, \Delta^{(j)})$ which generates a source task $\mathcal{T}^{(j)}$ by editing a set of states $\Delta^{(j)} \subseteq \mathbf{V}$ in the target task \mathcal{T} . It follows a reverse topological ordering over actions $\mathbf{X} = \{X_1, \dots, X_H\}$. For every step $j = H, \dots, 1$, the algorithm call the subroutine FINDMAXEDIT (Algo. 1) to find a set of editable states $\Delta^{(j)}$ w.r.t. actions $\mathbf{X}^{(j)} = \{X_j, \dots, X_H\}$. It then calls the generator GEN to generate a source task $\mathcal{T}^{(j)}$ by editing states $\Delta^{(j)}$. The conditions in Thm. 3 ensure that Algo. 3 returns a causally aligned curriculum.

Corollary 1. For a soluble target task $\mathcal{T} = \langle \mathcal{M}, \Pi, \mathcal{R} \rangle$, let \mathcal{G}_π be an intervened causal diagram of \mathcal{M} . $\text{FINDCAUSALCURRICULUM}(\mathcal{T}, \mathcal{G}_\pi)$ returns a causally aligned curriculum.

A more detailed discussion on the additional conditions under which a combination of Algs. 2 and 3 is guaranteed to find an optimal target task policy is provided in App. D.

Algorithm 3: FINDCAUSALCURRICULUM

Input: A target task \mathcal{T} , a causal diagram \mathcal{G}_π

Output: A causally aligned curriculum \mathcal{C}

Let $\mathcal{C} \leftarrow \emptyset$;

for $j = H, \dots, 1$ **do**

Let $\mathbf{X}^{(j)} \leftarrow \{X_j, \dots, X_H\}$;

Let $\Delta^{(j)} \leftarrow \text{FINDMAXEDIT}(\mathcal{G}_\pi, \mathbf{X}^{(j)})$;

Let $\mathcal{T}^{(j)} \leftarrow \text{GEN}(\mathcal{T}, \Delta^{(j)})$;

Let $\mathcal{C} = \mathcal{C} \cup \{\mathcal{T}^{(j)}\}$;

return \mathcal{C} ;

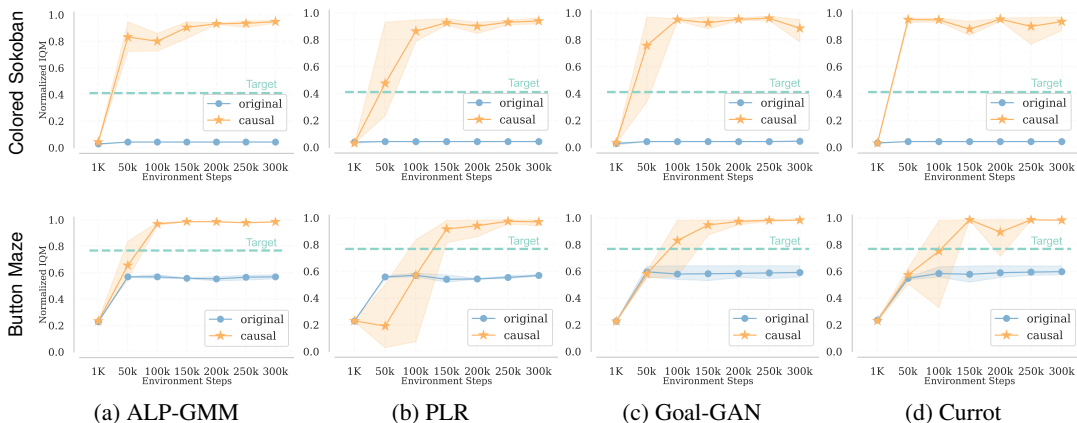


Figure 5: Target task performance of the agents at different training stages in Colored Sokoban (Row 1) and Button Maze (Row 2) using different curriculum generators (Columns). The horizontal green line shows the performance of the agent trained directly in the target. “original” refers to the unaugmented curriculum generator and “causal” refers to its causally augmented version.

4 EXPERIMENTS

In this section, we build on Algo. 3 and different curriculum generators to evaluate causally aligned curricula for solving challenging tasks in which confounding bias is present and previous, non-causal generators cannot solve. In particular, we test four best-performing curriculum generators: ALP-GMM (Portelas et al., 2019), PLR (Jiang et al., 2021), Goal-GAN (Florensa et al., 2018), and Currot (Klink et al., 2022) in two confounded environments with pixel observations: (a) Colored Sokoban, (b) Button Maze. All experiments are conducted with five random seeds and reported in Interquartile Mean (IQM) normalized w.r.t the minimum and maximum rewards with 95% confidence intervals shown in shades. See App. F for detailed specifications and more results.

Colored Sokoban. Consider the same Sokoban game as shown in Example 1. The curriculum generators are allowed to vary the initial location of the agent, to vary the initial box location, and to intervene the box’s color. Without editing, the box color syncs with the true underlying rewards, i.e., pushing a yellow box always yields a positive reward. However, after intervening the box color, this sync is broken and the agent has no information on the right time to push the box. As shown in Fig. 5 agents trained by original curriculum generators failed to converge due to this. After causal augmentation, those misaligned source tasks with intervened box color are all eliminated from the search space during curriculum generation. The causal versions of those generators successfully train the agent to converge efficiently and surpass the performance of those trained directly in the target task.

Button Maze. In this grid world environment (Chevalier-Boisvert et al., 2018), the agent must navigate to the goal location and step onto it at the right time. Specifically, after pushing the button, the goal region will turn green and yield a positive reward if the agent steps onto it. However, before pushing the button, there is only a 20% chance the agent gets a positive reward for reaching the goal, and the goal randomly blinks between red and green, independent of the underlying rewards. Curriculum generators can intervene the goal color and vary the agent’s initial location but intervening goal colors creates misaligned curricula (Thm. 3). As shown in Fig. 5 agents trained by vanilla curriculum generators failed to learn at all, while the agents trained by their causally-augmented versions all converged to the optimal, even surpassing the one trained directly in the target task.

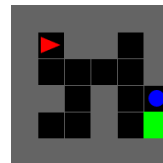


Figure 6: Button Maze.

5 CONCLUSION

We develop a formal treatment for automatic curriculum design in confounded environments through causal lenses. We propose a sufficient graphical criterion that edits must conform with so as to generate causally aligned source tasks in which the agent is guaranteed to learn optimal decision

rules for the target task. We also develop a practical implementation of our graphical criteria, i.e., FINDMAXEDIT, that augments the existing curriculum generators into ones that generate aligned source tasks regardless of the existence of unobserved confounders. Finally, we analyze causally aligned curricula’ design principles with theoretical performance guarantees. The effectiveness of our approach is empirically verified in two high-dimensional pixel-based tasks.

ACKNOWLEDGEMENTS

This research was supported in part by the NSF, ONR, AFOSR, DoE, Amazon, JP Morgan, and The Alfred P. Sloan Foundation.

REPRODUCIBILITY STATEMENT

For all the theorems, corollaries, and algorithms, we provide proofs and correctness analysis in App. E. To implement the algorithms, we provide pseudo-code in the main text and App. C. We also provide experiment specifications, environment setup, and neural network hyperparameters in App. F. Colored Sokoban and Button Maze are implemented based on Sokoban (Schrader, 2018) and GridWorld (Chevalier-Boisvert et al., 2018), respectively.

REFERENCES

- David Abel, Will Dabney, Anna Harutyunyan, Mark K Ho, Michael Littman, Doina Precup, and Satinder Singh. On the expressivity of markov reward. *Advances in Neural Information Processing Systems*, 34:7799–7812, 2021.
- Rishabh Agarwal, Max Schwarzer, Pablo Samuel Castro, Aaron Courville, and Marc G Belle-mare. Deep reinforcement learning at the edge of the statistical precipice. In A. Beygelzimer, Y. Dauphin, P. Liang, and J. Wortman Vaughan (eds.), *Advances in Neural Information Processing Systems*, 2021. URL <https://openreview.net/forum?id=uqv8-U4lKBe>.
- Jacob Andreas, Dan Klein, and Sergey Levine. Modular multitask reinforcement learning with policy sketches. In Doina Precup and Yee Whye Teh (eds.), *Proceedings of the 34th International Conference on Machine Learning, ICML 2017, Sydney, NSW, Australia, 6-11 August 2017*, volume 70 of *Proceedings of Machine Learning Research*, pp. 166–175. PMLR, 2017. URL <http://proceedings.mlr.press/v70/andreas17a.html>.
- Marcin Andrychowicz, Dwight Crow, Alex Ray, Jonas Schneider, Rachel Fong, Peter Welinder, Bob McGrew, Josh Tobin, Pieter Abbeel, and Wojciech Zaremba. Hindsight experience replay. In Isabelle Guyon, Ulrike von Luxburg, Samy Bengio, Hanna M. Wallach, Rob Fergus, S. V. N. Vishwanathan, and Roman Garnett (eds.), *Advances in Neural Information Processing Systems 30: Annual Conference on Neural Information Processing Systems 2017, December 4-9, 2017, Long Beach, CA, USA*, pp. 5048–5058, 2017. URL <https://proceedings.neurips.cc/paper/2017/hash/453fadbd8ala3af50a9df4df899537b5-Abstract.html>.
- Minoru Asada, Shoichi Noda, Sukoya Tawaratsumida, and Koh Hosoda. Purposive behavior acquisition for a real robot by vision-based reinforcement learning. *Machine Learning*, 23(2-3): 279–303, 1996. doi: 10.1023/A:1018237008823. URL <https://doi.org/10.1023/A:1018237008823>.
- Adrien Baranes and Pierre-Yves Oudeyer. Active learning of inverse models with intrinsically motivated goal exploration in robots. *Robotics and Autonomous Systems*, 61(1):49–73, 2013. doi: 10.1016/j.robot.2012.05.008. URL <https://doi.org/10.1016/j.robot.2012.05.008>.
- Elias Bareinboim and Judea Pearl. Causal inference and the data-fusion problem. *Proceedings of the National Academy of Sciences*, 113(27):7345–7352, 2016. doi: 10.1073/pnas.1510507113. URL <https://www.pnas.org/doi/abs/10.1073/pnas.1510507113>

-
- Elias Bareinboim, Juan D. Correa, Duligur Ibeling, and Thomas Icard. *On Pearl's Hierarchy and the Foundations of Causal Inference*, pp. 507–556. Association for Computing Machinery, New York, NY, USA, 1 edition, 2022. ISBN 9781450395861. URL <https://doi.org/10.1145/3501714.3501743>
- Marc G. Bellemare, Sriram Srinivasan, Georg Ostrovski, Tom Schaul, David Saxton, and Rémi Munos. Unifying count-based exploration and intrinsic motivation. In Daniel D. Lee, Masashi Sugiyama, Ulrike von Luxburg, Isabelle Guyon, and Roman Garnett (eds.), *Advances in Neural Information Processing Systems 29: Annual Conference on Neural Information Processing Systems 2016, December 5-10, 2016, Barcelona, Spain*, pp. 1471–1479, 2016. URL <https://proceedings.neurips.cc/paper/2016/hash/afda332245e2af431fb7b672a68b659d-Abstract.html>
- Richard Bellman. Dynamic programming. *Science*, 153(3731):34–37, 1966. doi: 10.1126/science.153.3731.34. URL <https://www.science.org/doi/abs/10.1126/science.153.3731.34>
- Yuri Burda, Harrison Edwards, Amos J. Storkey, and Oleg Klimov. Exploration by random network distillation. In *7th International Conference on Learning Representations, ICLR 2019, New Orleans, LA, USA, May 6-9, 2019*. OpenReview.net, 2019. URL <https://openreview.net/forum?id=H11JjNR5Ym>
- Maxime Chevalier-Boisvert, Lucas Willems, and Suman Pal. Minimalistic gridworld environment for gymnasium, 2018. URL <https://github.com/Farama-Foundation/Minigrid>
- Daesol Cho, Seungjae Lee, and H. Jin Kim. Outcome-directed reinforcement learning by uncertainty & temporal distance-aware curriculum goal generation. In *The Eleventh International Conference on Learning Representations*, 2023. URL <https://openreview.net/forum?id=v69itrHLEu>
- Juan Correa and Elias Bareinboim. General transportability of soft interventions: Completeness results. In H. Larochelle, M. Ranzato, R. Hadsell, M.F. Balcan, and H. Lin (eds.), *Advances in Neural Information Processing Systems*, volume 33, pp. 10902–10912. Curran Associates, Inc., 2020. URL https://proceedings.neurips.cc/paper_files/paper/2020/file/7b497aalb2a83ec63d1777a88676b0c2-Paper.pdf
- Steve Dahlsgog and Julian Togelius. A multi-level level generator. In *2014 IEEE Conference on Computational Intelligence and Games, CIG 2014, Dortmund, Germany, August 26-29, 2014*, pp. 1–8. IEEE, 2014. doi: 10.1109/CIG.2014.6932909. URL <https://doi.org/10.1109/CIG.2014.6932909>
- Michael Dennis, Natasha Jaques, Eugene Vinitsky, Alexandre M. Bayen, Stuart Russell, Andrew Critch, and Sergey Levine. Emergent complexity and zero-shot transfer via unsupervised environment design. In Hugo Larochelle, Marc’Aurelio Ranzato, Raia Hadsell, Maria-Florina Balcan, and Hsuan-Tien Lin (eds.), *Advances in Neural Information Processing Systems 33: Annual Conference on Neural Information Processing Systems 2020, NeurIPS 2020, December 6-12, 2020, Virtual*, 2020. URL <https://proceedings.neurips.cc/paper/2020/hash/985e9a46e10005356bbaf194249f6856-Abstract.html>
- Adrien Ecoffet, Joost Huizinga, Joel Lehman, Kenneth O. Stanley, and Jeff Clune. Go-explore: a new approach for hard-exploration problems. arxiv, 2019. URL <http://arxiv.org/abs/1901.10995>
- Benjamin Eysenbach, Abhishek Gupta, Julian Ibarz, and Sergey Levine. Diversity is all you need: Learning skills without a reward function. In *7th International Conference on Learning Representations, ICLR 2019, New Orleans, LA, USA, May 6-9, 2019*. OpenReview.net, 2019. URL <https://openreview.net/forum?id=SJx63jRqFm>
- Carlos Florensa, David Held, Markus Wulfmeier, Michael Zhang, and Pieter Abbeel. Reverse curriculum generation for reinforcement learning. In *1st Annual Conference on Robot Learning, CoRL 2017, Mountain View, California, USA, November 13-15, 2017, Proceedings*, volume 78 of *Proceedings of Machine Learning Research*, pp. 482–495. PMLR, 2017. URL <http://proceedings.mlr.press/v78/florensa17a.html>

-
- Carlos Florensa, David Held, Xinyang Geng, and Pieter Abbeel. Automatic goal generation for reinforcement learning agents. In Jennifer G. Dy and Andreas Krause (eds.), *Proceedings of the 35th International Conference on Machine Learning, ICML 2018, Stockholm, Sweden, July 10-15, 2018*, volume 80 of *Proceedings of Machine Learning Research*, pp. 1514–1523. PMLR, 2018. URL <http://proceedings.mlr.press/v80/florensa18a.html>.
- Xing Hu, Rui Zhang, Ke Tang, Jiaming Guo, Qi Yi, Ruizhi Chen, Zidong Du, Ling Li, Qi Guo, Yunji Chen, et al. Causality-driven hierarchical structure discovery for reinforcement learning. *Advances in Neural Information Processing Systems*, 35:20064–20076, 2022.
- Peide Huang, Mengdi Xu, Jiacheng Zhu, Laixi Shi, Fei Fang, and Ding Zhao. Curriculum reinforcement learning using optimal transport via gradual domain adaptation. In Alice H. Oh, Alekh Agarwal, Danielle Belgrave, and Kyunghyun Cho (eds.), *Advances in Neural Information Processing Systems*, 2022a. URL https://openreview.net/forum?id=_cFdPHRLuJ
- Shengyi Huang, Rousslan Fernand Julien Dossa, Antonin Raffin, Anssi Kanervisto, and Weixun Wang. The 37 implementation details of proximal policy optimization. In *ICLR Blog Track*, 2022b. URL <https://iclr-blog-track.github.io/2022/03/25/ppo-implementation-details/> <https://iclr-blog-track.github.io/2022/03/25/ppo-implementation-details/>.
- Shengyi Huang, Rousslan Fernand Julien Dossa, Chang Ye, Jeff Braga, Dipam Chakraborty, Kinal Mehta, and João G.M. Araújo. Cleanrl: High-quality single-file implementations of deep reinforcement learning algorithms. *Journal of Machine Learning Research*, 23(274):1–18, 2022c. URL <http://jmlr.org/papers/v23/21-1342.html>.
- Minqi Jiang, Edward Grefenstette, and Tim Rocktäschel. Prioritized level replay. In Marina Meila and Tong Zhang (eds.), *Proceedings of the 38th International Conference on Machine Learning, ICML 2021, 18-24 July 2021, Virtual Event*, volume 139 of *Proceedings of Machine Learning Research*, pp. 4940–4950. PMLR, 2021. URL <http://proceedings.mlr.press/v139/jiang21b.html>.
- Niels Justesen, Ruben Rodriguez Torrado, Philip Bontrager, Ahmed Khalifa, Julian Togelius, and Sebastian Risi. Illuminating generalization in deep reinforcement learning through procedural level generation. In *Advances in Neural Information Processing Systems 31: Annual Conference on Neural Information Processing Systems 2018, NeurIPS 2018, December 3-8, 2018, Montréal, Canada*, 2018. URL <https://doi.org/10.48550/arXiv.1806.10729>.
- Leslie Pack Kaelbling, Michael L Littman, and Andrew W Moore. Reinforcement learning: A survey. *Journal of artificial intelligence research*, 4:237–285, 1996.
- Leslie Pack Kaelbling, Michael L Littman, and Anthony R Cassandra. Planning and acting in partially observable stochastic domains. *Artificial intelligence*, 101(1-2):99–134, 1998.
- Faisal Khan, Xiaojin (Jerry) Zhu, and Bilge Mutlu. How do humans teach: On curriculum learning and teaching dimension. In John Shawe-Taylor, Richard S. Zemel, Peter L. Bartlett, Fernando C. N. Pereira, and Kilian Q. Weinberger (eds.), *Advances in Neural Information Processing Systems 24: 25th Annual Conference on Neural Information Processing Systems 2011. Proceedings of a meeting held 12-14 December 2011, Granada, Spain*, pp. 1449–1457, 2011. URL <https://proceedings.neurips.cc/paper/2011/hash/f9028faec74be6ec9b852b0a542e2f39-Abstract.html>
- Pascal Klink, Haoyi Yang, Carlo D’Eramo, Jan Peters, and Joni Pajarinen. Curriculum reinforcement learning via constrained optimal transport. In Kamalika Chaudhuri, Stefanie Jegelka, Le Song, Csaba Szepesvári, Gang Niu, and Sivan Sabato (eds.), *International Conference on Machine Learning, ICML 2022, 17-23 July 2022, Baltimore, Maryland, USA*, volume 162 of *Proceedings of Machine Learning Research*, pp. 11341–11358. PMLR, 2022. URL <https://proceedings.mlr.press/v162/klink22a.html>
- Daphne Koller and Nir Friedman. *Probabilistic Graphical Models - Principles and Techniques*. MIT Press, 2009. ISBN 978-0-262-01319-2. URL <http://mitpress.mit.edu/catalog/item/default.asp?tttype=2&tid=11886>

-
- Daphne Koller and Brian Milch. Multi-agent influence diagrams for representing and solving games. *Games and Economic Behavior*, 45(1):181–221, 2003. doi: 10.1016/S0899-8256(02)00544-4. URL [https://doi.org/10.1016/S0899-8256\(02\)00544-4](https://doi.org/10.1016/S0899-8256(02)00544-4)
- Steffen L Lauritzen and Dennis Nilsson. Representing and solving decision problems with limited information. *Management Science*, 47(9):1235–1251, 2001.
- Adam Li, Amin Jaber, and Elias Bareinboim. Causal discovery from observational and interventional data across multiple environments. In *Thirty-seventh Conference on Neural Information Processing Systems*, 2023. URL <https://openreview.net/forum?id=C9wTM5xyw2>
- Diego Perez Liebana, Spyridon Samothrakis, Julian Togelius, Tom Schaul, and Simon M. Lucas. General video game AI: competition, challenges and opportunities. In Dale Schuurmans and Michael P. Wellman (eds.), *Proceedings of the Thirtieth AAAI Conference on Artificial Intelligence, February 12-17, 2016, Phoenix, Arizona, USA*, pp. 4335–4337. AAAI Press, 2016. URL <http://www.aaai.org/ocs/index.php/AAAI/AAAI16/paper/view/11853>
- Patrick MacAlpine and Peter Stone. Overlapping layered learning. *Artificial Intelligence*, 254: 21–43, 2018. doi: 10.1016/j.artint.2017.09.001. URL <https://doi.org/10.1016/j.artint.2017.09.001>
- Sanmit Narvekar, Jivko Sinapov, Matteo Leonetti, and Peter Stone. Source task creation for curriculum learning. In Catholijn M. Jonker, Stacy Marsella, John Thangarajah, and Karl Tuyls (eds.), *Proceedings of the 2016 International Conference on Autonomous Agents & Multiagent Systems, Singapore, May 9-13, 2016*, pp. 566–574. ACM, 2016. URL <http://dl.acm.org/citation.cfm?id=2937007>
- Sanmit Narvekar, Jivko Sinapov, and Peter Stone. Autonomous task sequencing for customized curriculum design in reinforcement learning. In Carles Sierra (ed.), *Proceedings of the Twenty-Sixth International Joint Conference on Artificial Intelligence, IJCAI 2017, Melbourne, Australia, August 19-25, 2017*, pp. 2536–2542. ijcai.org, 2017. doi: 10.24963/ijcai.2017/353. URL <https://doi.org/10.24963/ijcai.2017/353>
- Sanmit Narvekar, Bei Peng, Matteo Leonetti, Jivko Sinapov, Matthew E. Taylor, and Peter Stone. Curriculum learning for reinforcement learning domains: A framework and survey. *Journal of Machine Learning Research*, 21:181:1–181:50, 2020. URL <http://jmlr.org/papers/v21/20-212.html>
- OpenAI, Ilge Akkaya, Marcin Andrychowicz, Maciek Chociej, Mateusz Litwin, Bob McGrew, Arthur Petron, Alex Paino, Matthias Plappert, Glenn Powell, Raphael Ribas, Jonas Schneider, Nikolas Tezak, Jerry Tworek, Peter Welinder, Lilian Weng, Qiming Yuan, Wojciech Zaremba, and Lei Zhang. Solving rubik’s cube with a robot hand. arxiv, 2019. URL <http://arxiv.org/abs/1910.07113>
- Jack Parker-Holder, Minqi Jiang, Michael Dennis, Mikayel Samvelyan, Jakob N. Foerster, Edward Grefenstette, and Tim Rocktäschel. Evolving curricula with regret-based environment design. In Kamalika Chaudhuri, Stefanie Jegelka, Le Song, Csaba Szepesvári, Gang Niu, and Sivan Sabato (eds.), *International Conference on Machine Learning, ICML 2022, 17-23 July 2022, Baltimore, Maryland, USA*, volume 162 of *Proceedings of Machine Learning Research*, pp. 17473–17498. PMLR, 2022. URL <https://proceedings.mlr.press/v162/parker-holder22a.html>
- Judea Pearl. *Causality: Models, Reasoning, and Inference*. Cambridge University Press, 2 edition, 2009. doi: 10.1017/CBO9780511803161.
- Judea Pearl and Elias Bareinboim. Transportability of Causal and Statistical Relations: A Formal Approach. In *Proceedings of the Twenty-Fifth AAAI Conference on Artificial Intelligence*, volume 25, pp. 247–254, 2011. doi: 10.1609/aaai.v25i1.7861. URL <https://ojs.aaai.org/index.php/AAAI/article/view/7861>
- Bei Peng, James MacGlashan, Robert Loftin, Michael L Littman, David L Roberts, and Matthew E Taylor. Curriculum design for machine learners in sequential decision tasks. *IEEE Transactions on Emerging Topics in Computational Intelligence*, 2(4):268–277, 2018. doi: 10.1109/TETCI.2018.2829980. URL <https://doi.org/10.1109/TETCI.2018.2829980>

-
- Ronan Perry, Julius Von Kügelgen, and Bernhard Schölkopf. Causal discovery in heterogeneous environments under the sparse mechanism shift hypothesis. In Alice H. Oh, Alekh Agarwal, Danielle Belgrave, and Kyunghyun Cho (eds.), *Advances in Neural Information Processing Systems*, 2022. URL <https://openreview.net/forum?id=kFRCvpubDJo>.
- Rémy Portelas, Cédric Colas, Katja Hofmann, and Pierre-Yves Oudeyer. Teacher algorithms for curriculum learning of Deep RL in continuously parameterized environments. In Leslie Pack Kaelbling, Danica Kragic, and Komei Sugiura (eds.), *3rd Annual Conference on Robot Learning, CoRL 2019, Osaka, Japan, October 30 - November 1, 2019, Proceedings*, volume 100 of *Proceedings of Machine Learning Research*, pp. 835–853. PMLR, 2019. URL <http://proceedings.mlr.press/v100/portelas20a.html>.
- Rémy Portelas, Cédric Colas, Lilian Weng, Katja Hofmann, and Pierre-Yves Oudeyer. Automatic curriculum learning for deep RL: A short survey. In Christian Bessiere (ed.), *Proceedings of the Twenty-Ninth International Joint Conference on Artificial Intelligence, IJCAI 2020*, pp. 4819–4825. ijcai.org, 2020. doi: 10.24963/ijcai.2020/671. URL <https://doi.org/10.24963/ijcai.2020/671>.
- Sébastien Racanière, Andrew K. Lampinen, Adam Santoro, David P. Reichert, Vlad Firoiu, and Timothy P. Lillicrap. Automated curricula through setter-solver interactions. arxiv, 2019. URL <http://arxiv.org/abs/1909.12892>.
- Sebastian Risi and Julian Togelius. Increasing generality in machine learning through procedural content generation. *Nature Machine Intelligence*, 2(8):428–436, 2020.
- Tim Salimans and Richard Chen. Learning montezuma’s revenge from a single demonstration. arxiv, 2018. URL <http://arxiv.org/abs/1812.03381>.
- Terence D Sanger. Neural network learning control of robot manipulators using gradually increasing task difficulty. *IEEE transactions on Robotics and Automation*, 10(3):323–333, 1994. doi: 10.1109/70.294207. URL <https://doi.org/10.1109/70.294207>.
- Tom Schaul. A video game description language for model-based or interactive learning. In *2013 IEEE Conference on Computational Intelligence in Games (CIG), Niagara Falls, ON, Canada, August 11-13, 2013*, pp. 1–8. IEEE, 2013. doi: 10.1109/CIG.2013.6633610. URL <https://doi.org/10.1109/CIG.2013.6633610>.
- Max-Philipp B. Schrader. Gym-sokoban, 2018. URL <https://github.com/mpSchrader/gym-sokoban>.
- John Schulman, Filip Wolski, Prafulla Dhariwal, Alec Radford, and Oleg Klimov. Proximal policy optimization algorithms. arxiv, 2017. URL <http://arxiv.org/abs/1707.06347>.
- Oliver G. Selfridge, Richard S. Sutton, and Andrew G. Barto. Training and tracking in robotics. In *Proceedings of the 9th International Joint Conference on Artificial Intelligence - Volume 1, IJCAI’85*, pp. 670–672. Morgan Kaufmann Publishers Inc., 1985. ISBN 0-934613-02-8.
- Felipe Leno Da Silva and Anna Helena Reali Costa. Object-oriented curriculum generation for reinforcement learning. In *Proceedings of the 17th International Conference on Autonomous Agents and MultiAgent Systems, AAMAS ’18*, pp. 1026–1034, Richland, SC, 2018. International Foundation for Autonomous Agents and Multiagent Systems.
- Satinder Singh, Andrew G. Barto, and Nuttapon Chentanez. Intrinsically motivated reinforcement learning. In *Advances in Neural Information Processing Systems 17 [Neural Information Processing Systems, NIPS 2004, December 13-18, 2004, Vancouver, British Columbia, Canada]*, volume 17, pp. 1281–1288, 2004. URL <https://proceedings.neurips.cc/paper/2004/hash/4be5a36cbaca8ab9d2066debfe4e65c1-Abstract.html>.
- Sainbayar Sukhbaatar, Zeming Lin, Ilya Kostrikov, Gabriel Synnaeve, Arthur Szlam, and Rob Fergus. Intrinsic motivation and automatic curricula via asymmetric self-play. In *6th International Conference on Learning Representations, ICLR 2018, Vancouver, BC, Canada, April 30 - May 3, 2018, Conference Track Proceedings*. OpenReview.net, 2018. URL <https://openreview.net/forum?id=SKT5Yg-RZ>.

-
- Richard S Sutton and Andrew G Barto. *Reinforcement Learning: An Introduction*. A Bradford Book, second edition, 2018. ISBN 0262039249.
- Maxwell Svetlik, Matteo Leonetti, Jivko Sinapov, Rishi Shah, Nick Walker, and Peter Stone. Automatic curriculum graph generation for reinforcement learning agents. In *Proceedings of the AAAI Conference on Artificial Intelligence*, volume 31, 2023/06/09 2017. doi: 10.1609/aaai.v31i1.10933. URL <https://ojs.aaai.org/index.php/AAAI/article/view/10933>
- Benito van der Zander, Maciej Liundekiewicz, and Johannes Textor. Constructing separators and adjustment sets in ancestral graphs. In *Proceedings of the UAI 2014 Conference on Causal Inference: Learning and Prediction - Volume 1274*, CI'14, pp. 11–24. CEUR-WS.org, 2014.
- Rui Wang, Joel Lehman, Jeff Clune, and Kenneth O. Stanley. Paired open-ended trailblazer (POET): endlessly generating increasingly complex and diverse learning environments and their solutions. arxiv, 2019. URL <http://arxiv.org/abs/1901.01753>
- Rui Wang, Joel Lehman, Aditya Rawal, Jiale Zhi, Yulun Li, Jeffrey Clune, and Kenneth O. Stanley. Enhanced POET: open-ended reinforcement learning through unbounded invention of learning challenges and their solutions. In *Proceedings of the 37th International Conference on Machine Learning, ICML 2020, 13-18 July 2020, Virtual Event*, volume 119 of *Proceedings of Machine Learning Research*, pp. 9940–9951. PMLR, 2020. URL <http://proceedings.mlr.press/v119/wang201.html>
- Junzhe Zhang and Elias Bareinboim. Designing optimal dynamic treatment regimes: A causal reinforcement learning approach. In Hal Daumé III and Aarti Singh (eds.), *Proceedings of the 37th International Conference on Machine Learning*, volume 119 of *Proceedings of Machine Learning Research*, pp. 11012–11022. PMLR, 13–18 Jul 2020. URL <https://proceedings.mlr.press/v119/zhang20a.html>

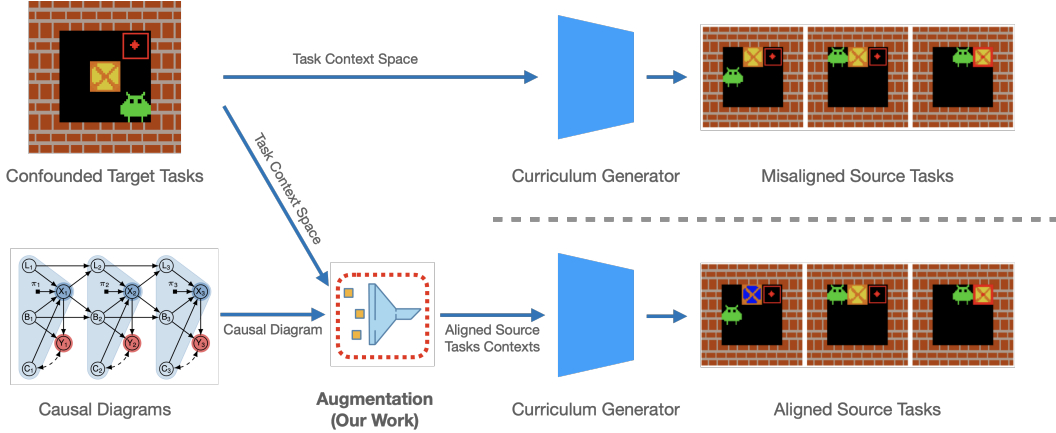


Figure 7: An overview of our proposed approach. In the upper half, the non-causal curriculum generator will produce misaligned source tasks failing to train the agent to convergence. While in our approach (the bottom half), we utilize the qualitative causal knowledge (causal diagrams) to filter out those misaligned source task contexts such that applying the same curriculum generator can now produce aligned source tasks.

APPENDICES

A METHOD OVERVIEW

In this section, we will summarize our proposed approach from a high-level view and provide a figure for better illustration of the pipeline.

B DETAILED COMPUTATIONS OF EXAMPLE 1

For the reward of pushing the box, we have,

$$\mathbb{E} [Y_i | B_i = \text{“next to goal”}, C_i; \text{do}(X_i = \text{“push”})] \quad (9)$$

$$= \mathbb{E} [Y_i | B_i = \text{“next to goal”}, U_i; \text{do}(X_i = \text{“push”})] \quad (10)$$

$$= 10 \times \mathbb{1}(U_i = 0) - 10 \times \mathbb{1}(U_i = 1) \quad (11)$$

$$= \begin{cases} 10 & \text{if } C_i = 0 \\ -10 & \text{if } C_i = 1 \end{cases} \quad (12)$$

After fixing the box color, we have,

$$\mathbb{E} [Y_i | B_i = \text{“next to goal”}; \text{do}(C_i, X_i = \text{“push”})] \quad (13)$$

$$= 10 \times P(U_i = 0) - 10 \times P(U_i = 1) \quad (14)$$

$$= -5. \quad (15)$$

C VARIATIONS OF ALGORITHMS

The first task of deciding editability is a direct application of the criterion in Def. 4 and can be implemented by using TESTSEP (Algo. 4). Finding an editable set and finding the maximal editable set are both solved by our proposed Algo. 1. After we find the maximal editable set, by Thm. 2 the power set of it is indeed all the possible editable sets w.r.t $\mathbf{X}^{(j)}$ in \mathcal{G}_π (Algo. 5). Note that there are exponentially many subsets so we focus on the time complexity of yielding each output. We implement this by bit manipulation. Specifically, we denote the existence of a variable in the output set as 0 or 1. Then listing all the elements in a power set of $\Delta^{(j)}$ is equivalent to decrease a bit mask from $2^{|\Delta^{(j)}|} - 1$ to 0. Each mask in this process represents a unique subset of $\Delta^{(j)}$.

Table 1: Time complexity of FINDMAXEDIT and its variations.

Algorithm	Description	Runtime
ISEEDIT	For given set of $\tau^{(j)}$, $\mathbf{X}^{(j)}$ and graph \mathcal{G}_π decide editability	$\mathcal{O}(d(n+m))$
FINDEDIT	Find an admissible set of $\tau^{(j)}$ w.r.t $\mathbf{X}^{(j)}$ in \mathcal{G}_π	$\mathcal{O}(dn^2)$
FINDMAXEDIT	Find the maximal admissible set of $\tau^{(j)}$ w.r.t $\mathbf{X}^{(j)}$ in \mathcal{G}_π	$\mathcal{O}(dn^2)$
LISTEDIT	List all admissible sets of $\tau^{(j)}$ w.r.t $\mathbf{X}^{(j)}$ in \mathcal{G}_π	$\mathcal{O}(n)$ delay

Algorithm 4: ISEEDIT

Input: A set of edit indicators $\tau^{(j)}$, a set of actions $\mathbf{X}^{(j)}$ and a graph \mathcal{G}_π .

Output: Whether the input edits are admissible.

```

for  $X$  in  $\mathbf{X}^{(j)}$  do
  | if  $(\tau^{(j)} \perp\!\!\!\perp \mathbf{Y} \cap De(X) \mid X, \mathbf{S}_X)$  in  $\mathcal{G}_\pi$  then
  | | return False;
return True;

```

D ALGORITHM FOR CAUSALLY ALIGNED CURRICULUM LEARNING

Algo. 3 construct the curriculum before any training is done. However, a more common practice is to construct the curriculum while adapting to the edge of the agent’s capability. In this section, we will discuss a more involved version of Algo. 3 that implements this idea. As we have seen in the main text, two source tasks $\mathcal{T}^{(i)}, \mathcal{T}^{(j)}$ in a soluble curriculum satisfy $\mathbf{X}^{(i)} \subseteq \mathbf{X}^{(j)}$ if $i < j$. This incremental nature of the action sets actually brings us opportunities to reduce further the computation of finding editable states. Thm. 4 reveals a nice property of $\mathbf{X}^{(j)}$ such that if a set of state variables, $\Delta^{(j)}$, is editable w.r.t an action X , it is also editable w.r.t any actions X' precedent to X in the soluble ordering, $X' \prec X$, i.e., $(X' \cap De(Y) \perp\!\!\!\perp \pi \mid X', \mathbf{S}_{X'})$ in \mathcal{G}_π where π is a new regime node pointing to X .

Theorem 4 (Expanded Action Sets). *Let $\mathcal{T} = \langle \mathcal{M}, \Pi, \mathcal{R} \rangle$ be a soluble target task and $\mathcal{T}^{(j)} = \langle \mathcal{M}, \Pi, \mathcal{R}, \Delta^{(j)} \rangle$ an aligned source task of \mathcal{T} . Then $\Delta^{(j)}$ is also editable w.r.t $\mathbf{X}^{(j)+} = \{X' \mid X' \prec X, X \in \mathbf{X}^{(j)}\}$.*

Thm. 4 implies that when checking editability w.r.t a set of actions, we only need to check w.r.t the single action that ranked highest in the soluble ordering (e.g., for actions $X_3 \prec X_2 \prec X_1$, finding the editable states for $\{X_1\}$ is equivalent to finding editable states for $\{X_i\}_{i=1}^3$).

Based on the above discussion and Algo. 1, we propose a causal curriculum learning algorithm (Algo. 6) to find the optimal target task policy given a curriculum generator GEN that generates source tasks by editing a given set of editable states $\Delta^{(j)}$. This algorithm resonates with the heuristics that the agent should be trained in a sequence of more challenging source tasks (Portelas et al., 2020; Narvekar et al., 2020). More specifically, after sorting the actions in the soluble ordering, the first generated source task only requires the agent to learn the optimal target policy of action X_N (Say the target task \mathcal{T} is an N -step one). The next stage of learning will be to grasp the optimal target policy of both action X_N and X_{N-1} , but since the agent has already learned the optimal policy of X_N previously. This won’t be too much harder for it. We will continue this procedure until the agent learns the optimal policy for all the actions in the target task. Algo. 6 is basically a combination of CURRICULUM LEARNING (Algo. 2) and FINDCAUSALCURRICULUM (Algo. 3) except that for each Δ , there will be multiple source tasks $\mathcal{T}^{(j)}$ being generated until $\Omega(\mathbf{S}_i; \pi^*) \subseteq \bigcup_{T^{(j)} \in \mathcal{C}[X_i]} \Omega(\mathbf{S}_i; \pi^*(\mathcal{C}))$ where $\Omega(\mathbf{S}_i; \pi^*)$ is the space of possible \mathbf{S}_i values in the target task under the optimal target task policy π^* , $\Omega(\mathbf{S}_i; \pi^*(\mathcal{C}))$ is the space of possible \mathbf{S}_i values in source tasks under policy $\pi^*(\mathcal{C})$ and $\mathcal{C}[X_i]$ is the set of source tasks $\mathcal{T}^{(j)}$ such that $X_i \in \mathbf{X}^{(j)}$. This condition ensures that the input space of an action X_i is thoroughly traversed during training in the curriculum. If this is satisfied, it means that the agent has learned the optimal decision rule for X_i in every possible situation in the target task, as we show formally in the following theorem.

Algorithm 5: LISTEDIT

Input: A causal diagram \mathcal{G}_π , a set of actions $\mathbf{X}^{(j)}$.

Output: All possible editable sets.

$\Delta^{(j)} \rightarrow \text{FINDMAXEDIT}(\mathcal{G}_\pi, \mathbf{X}^{(j)});$

mask $\leftarrow 2^{|\Delta^{(j)}|} - 1;$

while mask **do**

$\Delta \leftarrow \emptyset;$

 tmpmask \leftarrow mask;

$i \leftarrow |\Delta^{(j)}| - 1;$

while tmpmask **do**

if tmpmask & 1 **then**

$\Delta \leftarrow \Delta \cup \{\Delta^{(j)}[i]\}$

$i \leftarrow i - 1;$

 tmpmask $\gg 1;$

 mask \leftarrow mask $- 1;$

yield $\Delta;$

Algorithm 6: CAUSAL CURRICULUM LEARNING

Input: A target task \mathcal{T} , a curriculum generator GEN.

Output: A policy trained in the curriculum \mathcal{C} , $\pi^*(\mathcal{C})$.

Generate causal diagram \mathcal{G}_π of \mathcal{T} w.r.t policy space Π ;

Sort the set of actions w.r.t the soluble ordering (ascending) and save the result into \mathbf{X}' ;

Randomly initialize the agent's policy $\pi^*(\mathcal{C})$;

$j \leftarrow 1;$

for X_i **in** \mathbf{X}' **do**

$\Delta \leftarrow \text{FINDMAXEDIT}(\mathcal{G}_\pi, \{X_i\});$

$\mathcal{C}[X_i] \leftarrow \emptyset;$

while $\Omega(\mathbf{S}_i; \pi^*) \not\subseteq \bigcup_{\mathcal{T}^{(j)} \in \mathcal{C}[X_i]} \Omega(\mathbf{S}_i; \pi^*(\mathcal{C}))$ **do**

 Generate source task $\mathcal{T}^{(j)}$ with GEN(\mathcal{T} , Δ);

 Train $\pi^*(\mathcal{C})$ in $\mathcal{T}^{(j)}$ to converge;

$\mathcal{C}[X_i] \leftarrow \mathcal{C}[X_i] \cup \{\mathcal{T}^{(j)}\};$

$j \leftarrow j + 1;$

return $\pi^*(\mathcal{C})$;

Theorem 5. *If the set of actions in target task satisfies $\mathbf{X} \subseteq \mathbf{X}^{(N)}$ and $\forall X_i \in \mathbf{X}, \Omega(\mathbf{S}_i; \pi^*) \subseteq \bigcup_{\mathcal{T}^{(j)} \in \mathcal{C}[X_i]} \Omega(\mathbf{S}_i; \pi^*(\mathcal{C}))$, the following solution $\pi^*(\mathcal{C})$ is an optimal policy π^* in the target task \mathcal{T} ,*

$$\pi^*(\mathcal{C}) = \arg \max_{\pi \in \Pi} \mathbb{E}_{\mathcal{M}^{(N)}} [\mathcal{R}(\mathbf{Y}); \pi], \quad (16)$$

where $\mathcal{M}^{(N)}$ is the SCM of source task $\mathcal{T}^{(N)}$, and $\mathcal{T}^{(N)}$ is aligned to \mathcal{T} w.r.t $\mathbf{X}^{(N)}$.

Nonetheless, there are other practical roadblocks before realizing optimal curriculum learning. For example, we don't have an exact measurement of when the input space of an action is traversed thoroughly by the curriculum, and the agent may not converge in every source task $\mathcal{T}^{(j)}$ to learn all the optimal decision rules of $\mathbf{X}^{(j)}$. But still, as we have shown in the experiments, simply augmenting the existing curriculum generators already gives us satisfying performance.

E PROOF FOR THEOREMS AND ALGORITHM CORRECTNESS

In this section, we provide proof sketches for all the theorems proposed in the previous sections.

Lemma 1. *If the set of edit indicators satisfy $(\tau^{(j)} \perp\!\!\!\perp \mathbf{Y}_X | X, \mathbf{S}_X)$ in a soluble source task, for any $X' \prec X$ in the soluble ordering, it satisfies $(\tau^{(j)} \perp\!\!\!\perp \mathbf{Y}_{X'} | X', \mathbf{S}_{X'})$.*

Proof of Lem. 7 We will prove this by contradiction. Suppose $(\tau^{(j)} \not\perp\!\!\!\perp \mathbf{Y}_{X'} | X', \mathcal{S}_{X'})$. There are three possibilities based on the type of node V to which $\tau^{(j)}$ corresponds.

- i) If $V \in \mathcal{S}_X$, we can show that the source task cannot be soluble by finding an open path from a pseudo parent of X to $\mathbf{Y}_{X'}$. Firstly, $X' \prec X$ in a soluble source task means $X' \in De(X)$. When adding a pseudo parent V' to X , the path $V' \rightarrow X \leftarrow V \leftarrow \tau^{(j)}$ is open under $X', \mathcal{S}_{X'}$. By the assumption, there also exists an open path from $\tau^{(j)}$ to $\mathbf{Y}_{X'}$ under $X', \mathcal{S}_{X'}$, which means that path $V' \rightarrow X \leftarrow V \leftarrow \tau^{(j)}$ is also open under $X', \mathcal{S}_{X'}$. Thus, this contradicts the definition of a soluble task and $X' \prec X$.
- ii) If $V \notin \mathcal{S}_X$ and $V \in An(X)$, we can find a similar open path as in the previous case. By the assumption, there exists an open path p from $\tau^{(j)}$ to $\mathbf{Y}_{X'}$ under $X', \mathcal{S}_{X'}$. But we have $X' \in De(X)$ and thus $\mathbf{Y}_{X'} \subseteq \mathbf{Y}_X$. This open path must be blocked under X, \mathcal{S}_X , which means that X must observe a non-collider variable Z on p . Without observing Z , p will be open under X, \mathcal{S}_X . Note that any colliders on p will have X' as their descendant since p is open under $X', \mathcal{S}_{X'}$, which creates new open paths. So, p won't be blocked because of colliders. Now, a pseudo parent of X , say V' , will again have an open path towards $\mathbf{Y}_{X'}$ under $X', \mathcal{S}_{X'}$, $V' \rightarrow X \leftarrow Z \cdots \rightarrow \mathbf{Y}_{X'}$, where $Z \cdots \rightarrow \mathbf{Y}_{X'}$ is part of the p path. Thus, this contradicts the definition of a soluble task and $X' \prec X$.
- iii) If $V \notin An(X)$, we prove contradictions by checking all the possible path types between V and $\mathbf{Y}_{X'}$. If the open path p from V to $\mathbf{Y}_{X'}$ under $X', \mathcal{S}_{X'}$ is causal, p must be blocked under X, \mathcal{S}_X by having X observe variables on p , which contradicts with the condition that $V \notin An(X)$. If p is not causal and there exist colliders, say Z , X' must be a descendant of such colliders. Let Z be the leftmost collider on p . This leads to another causal path p' , $\tau^{(j)} \rightarrow V \rightarrow \cdots \rightarrow Z \rightarrow \cdots \rightarrow X' \rightarrow \cdots \rightarrow \mathbf{Y}_{X'}$. Clearly, X cannot block p' by observing any variables on it. Thus, p' is open under X, \mathcal{S}_X which contradicts with the condition that $(\tau^{(j)} \perp\!\!\!\perp \mathbf{Y}_X | X, \mathcal{S}_X)$.

Thus, we have proved that if $(\tau^{(j)} \perp\!\!\!\perp \mathbf{Y}_X | X, \mathcal{S}_X)$ in a soluble source task, for any $X' \prec X$, it also satisfies $(\tau^{(j)} \perp\!\!\!\perp \mathbf{Y}_{X'} | X', \mathcal{S}_{X'})$. \square

Proof of Thm. 7 By definition, the optimal policy of the target task satisfies,

$$\pi^* = \arg \max_{\pi \in \Pi} \mathbb{E}_{\mathcal{M}} [\mathcal{R}(\mathbf{Y}); \pi]. \quad (17)$$

Similar definitions hold for the optimal policy $\pi^{(j)}$ of a source task $\mathcal{T}^{(j)}$. Our goal is to show that once the graphical criterion holds for $\tau^{(j)}$ and action X_i , the optimal decision rule of X_i on those shared input states of the source task and the target task is the same in these two tasks. We first simplify the calculation of the optimal decision rule at action X_i using the concept of ‘‘relevance graph’’ (Koller & Milch 2003).

Definition 8 (Relevance Graph of Tasks). The relevance graph, \mathcal{G}_r , of a target task $\mathcal{T} = \langle \mathcal{M}, \Pi, \mathcal{R} \rangle$ is a directed graph whose nodes representing action variables $\mathbf{X} \subseteq \mathbf{V}$ are connected by directed edges $X' \rightarrow X$ if and only if $(\pi' \not\perp\!\!\!\perp \mathbf{Y} \cap De(\mathbf{X}) | \mathcal{S}_X, X)$ where π' is an added regime node pointing to X' .

This relevance graph specifies the order in which those actions should be optimized. Intuitively, X' is optimized before X because it can affect X 's reward signal while X 's inputs, \mathcal{S}_X , and X itself cannot block such causal effects. We denote the topological order over actions in \mathcal{G}_r by \prec where $X' \prec X$ if and only if X' should be optimized before X . It is also possible that the relevance graph contains Strongly Connected Components (SCCs) where each pair of actions in the same SCC is connected by a directed path. Semantically, actions in the same SCC affect the rewards of each other. Thus, one must consider all actions in the same SCC to find the optimal policy for these actions (Koller & Milch 2003). Formally speaking, let \mathcal{L} be an equivalence relationship over \mathbf{X} such that action $X, X' \in \mathbf{X}$ belong to the same partition, $X \sim_{\mathcal{L}} X'$, (equivalently, $X \in [X']_{\mathcal{L}}$ or $X' \in [X]_{\mathcal{L}}$) if and only if they are in the same maximal SCC of a target task \mathcal{T} 's relevance graph, \mathcal{G}_r .⁴ When there is no SCC in the relevance graph, we say this target task is soluble Def. 7 which can be solved by a series of dynamic programs (Koller & Milch 2003; Lauritzen & Nilsson

⁴for simplicity, we will use $[X]$ to denote $[X]_{\mathcal{L}}$ in the following discussion.

[2001]). When there is an SCC, we can treat each SCC as a single high-level action taking value as the combination of all the actions in that SCC, i.e., $\Omega([X_i]) = \times_{X \in [X_i]} \Omega(X)$. After eliminating all such SCCs in the relevance graph, we transform the task back to a soluble one. So, the same solver can be used. Now we show that given an optimal target task policy, the decision rule at $[X_i]$ is optimal if and only if for every input $\mathbf{s}_{[X_i]} \in \Omega(\mathcal{S}_{[X_i]}; \pi^*)$,

$$\pi_{[X_i]}^*(\cdot | \mathbf{s}_{[X_i]}) = \arg \max_{\pi_{[X_i]}(\cdot | \mathbf{s}_{[X_i]})} \mathbb{E}_{\mathcal{M}} \left[\mathcal{R}(\mathbf{Y}_{[X_i]} | \mathbf{s}_{[X_i]}; \pi_{[X_i]} \cup \pi_{\prec[X_i]}^*) \right], \quad (18)$$

where $\mathbf{Y}_{[X_i]} = De([X_i]) \cap \mathbf{Y}$ is the set of rewards that are descendants of actions in the SCC of X_i and $\pi_{\succeq X_i}^*$ is the set of optimal decision rules of actions that precede $[X_i]$ w.r.t the relevance graph. By definition, the decision rule at $[X_i]$ is optimal if it maximizes the expected reward function when other parts of the optimal policy are given,

$$\pi_{[X_i]}^* = \arg \max_{\pi_{[X_i]}} \mathbb{E}_{\mathcal{M}} \left[\mathcal{R}(\mathbf{Y}); \pi_{[X_i]} \cup (\pi^* \setminus \pi_{[X_i]}^*) \right]. \quad (19)$$

We can expand the expected reward as follows,

$$\mathbb{E}_{\mathcal{M}} \left[\mathcal{R}(\mathbf{Y}); \pi_{[X_i]} \cup (\pi^* \setminus \pi_{[X_i]}^*) \right] = \sum_{\mathbf{s}_{[X_i]}} P(\mathbf{s}_{[X_i]}) \mathbb{E}_{\mathcal{M}} \left[\mathcal{R}(\mathbf{Y}) | \mathbf{s}_{[X_i]}; \pi_{[X_i]} \cup (\pi^* \setminus \pi_{[X_i]}^*) \right]. \quad (20)$$

Clearly, the input distribution of $\mathcal{S}_{[X_i]}$ is fixed given other parts of the optimal policy so Eq. (19) is equivalent to for every input $\mathbf{s}_{[X_i]} \in \Omega(\mathcal{S}_{[X_i]}; \pi^*)$,

$$\pi_{[X_i]}^*(\cdot | \mathbf{s}_{[X_i]}) = \arg \max_{\pi_{[X_i]}(\cdot | \mathbf{s}_{[X_i]})} \mathbb{E}_{\mathcal{M}} \left[\mathcal{R}(\mathbf{Y}) | \mathbf{s}_{[X_i]}; \pi_{[X_i]} \cup (\pi^* \setminus \pi_{[X_i]}^*) \right] \quad (21)$$

$$= \arg \max_{\pi_{[X_i]}(\cdot | \mathbf{s}_{[X_i]})} \sum_{\mathbf{y}_{[X_i]}} \mathcal{R}(\mathbf{y}) P(\mathbf{y} | \mathbf{s}_{[X_i]}, [x_i]; \pi^* \setminus \pi_{[X_i]}^*) \pi([x_i] | \mathbf{s}_{[X_i]}). \quad (22)$$

Since non-descendants of $[X_i]$ are independent of $[X_i]$ given $\mathcal{S}_{[X_i]}$ and actions are not confounded, we can further reduce the reward function to focus on only $\mathbf{Y}_{[X_i]}$, rewards that are descendants of $[X_i]$, assuming that $\mathcal{R}(\cdot)$ is cumulative,

$$\pi_{[X_i]}^*(\cdot | \mathbf{s}_{[X_i]}) = \arg \max_{\pi_{[X_i]}(\cdot | \mathbf{s}_{[X_i]})} \sum_{\mathbf{y}_{[X_i], [x_i]}} \mathcal{R}(\mathbf{y}_{[X_i]}) P(\mathbf{y}_{[X_i]} | \mathbf{s}_{[X_i]}, [x_i]; \pi^* \setminus \pi_{[X_i]}^*) \pi([x_i] | \mathbf{s}_{[X_i]}). \quad (23)$$

From the relevance graph definition, we know that only actions that precede $[X_i]$ in the relevance graph will affect $\mathbf{Y}_{[X_i]}$ given $\mathcal{S}_{[X_i]}, [X_i]$. Thus, we can simplify the conditioning further,

$$\pi_{[X_i]}^*(\cdot | \mathbf{s}_{[X_i]}) = \arg \max_{\pi_{[X_i]}(\cdot | \mathbf{s}_{[X_i]})} \sum_{\mathbf{y}_{[X_i], [x_i]}} \mathcal{R}(\mathbf{y}_{[X_i]}) P(\mathbf{y}_{[X_i]} | \mathbf{s}_{[X_i]}, [x_i]; \pi_{\prec[X_i]}^*) \pi([x_i] | \mathbf{s}_{[X_i]}) \quad (24)$$

$$= \arg \max_{\pi_{[X_i]}(\cdot | \mathbf{s}_{[X_i]})} \mathbb{E}_{\mathcal{M}} \left[\mathcal{R}(\mathbf{Y}_{[X_i]} | \mathbf{s}_{[X_i]}; \pi_{[X_i]} \cup \pi_{\prec[X_i]}^*) \right], \quad (25)$$

which is exactly Eq. (18). We can do a similar derivation for the optimal decision rule at $[X_i]$ in source task $\mathcal{T}^{(j)}$, for every input $\mathbf{s}_{[X_i]} \in \Omega^{(j)}(\mathcal{S}_{[X_i]}; \pi^{(j)})$,

$$\pi_{[X_i]}^{(j)}(\cdot | \mathbf{s}_{[X_i]}) = \arg \max_{\pi_{[X_i]}(\cdot | \mathbf{s}_{[X_i]})} \sum_{\mathbf{y}_{[X_i], [x_i]}} \mathcal{R}(\mathbf{y}_{[X_i]}) P(\mathbf{y}_{[X_i]} | \mathbf{s}_{[X_i]}, [x_i], \tau^{(j)}; \pi_{\prec[X_i]}^{(j)}) \pi([x_i] | \mathbf{s}_{[X_i]}) \quad (26)$$

$$= \arg \max_{\pi_{[X_i]}(\cdot | \mathbf{s}_{[X_i]})} \mathbb{E}_{\mathcal{M}^{(j)}} \left[\mathcal{R}(\mathbf{Y}_{[X_i]} | \mathbf{s}_{[X_i]}; \pi_{[X_i]} \cup \pi_{\prec[X_i]}^{(j)}) \right], \quad (27)$$

where $\tau^{(j)}$ is the edit indicator $\pi^{(j)}$ is the optimal policy of source task $\mathcal{T}^{(j)}$. In practice, we can let actions in each SCC X_i have an edge into every reward node associated with the SCC and still the graph is compatible with the original task. Then, we only need to show that once the graphical criterion is satisfied in such a graph, for any input $\mathbf{s}_i \in \Omega^{(j)}(\mathcal{S}_i; \pi^{(j)}) \cap \Omega(\mathcal{S}_i; \pi^*)$, the following holds,

$$P(\mathbf{y}_{X_i} | \mathbf{s}_{[X_i]}, [x_i]; \pi_{\prec[X_i]}^*) = P(\mathbf{y}_{X_i} | \mathbf{s}_{[X_i]}, [x_i], \tau^{(j)}; \pi_{\prec[X_i]}^{(j)}). \quad (28)$$

If this is true, the optimal decision rule at X_i will be invariant across both the target task and the source task. We first consider the simpler case when there is no SCC in the relevance graph. So, $[X_i] = \{X_i\}$. In this case, we can apply the result of Lem. 1 directly and know that the graphical criterion is also satisfied by any action $X \prec X_i$. Then we prove Eq. (28) holds by induction on action X_i . The base case is there is no action preceding X_i in the relevance graph. So, there will be no policy dependencies in Eq. (28), and it will be trivially true given the graphical criterion. Now we assume when there are k actions preceding X_i in the relevance graph, and the graphical criterion holds, Eq. (28) will hold. When there are $k + 1$ actions preceding X_i in the relevance graph, by the inductive hypothesis and the fact that graphical criterion also holds for $X \prec X_i$ when it holds for X_i , we know the optimal decision rules of $X \prec X_i$ stay the same across the source task and the target task. Thus, Eq. (28) is reduced to $P(\mathbf{y}_{X_i} | \mathbf{s}_{X_i}, x_i) = P(\mathbf{y}_{X_i} | \mathbf{s}_{X_i}, x_i, \tau^{(j)})$, which is true when the graphical criterion holds, $(\tau^{(j)} \perp\!\!\!\perp \mathbf{Y}_{X_i} | X_i, \mathbf{S}_i)$ in \mathcal{G}_π .

When there are SCCs in the relevance graph, the graphical criterion only shows us that $(\tau^{(j)} \perp\!\!\!\perp \mathbf{Y}_{X_i} | \mathbf{S}_i, X_i)$ in \mathcal{G}_π . But we can show that $(\tau^{(j)} \perp\!\!\!\perp \mathbf{Y}_{X_i} | [X_i], \mathbf{S}_{[X_i]})$ in \mathcal{G}_π also holds. Notice that the difference between these two criteria is that the latter includes more variables in the conditioning set. If the latter one doesn't hold, that means adding these variables opens up at least a collider path p that is blocked under the original criterion. Say this collider on p is M , and it's ancestral to an action $X_j \in [X_i]$. Clearly, there is an active path from $\tau^{(j)}$ to M and there is also an active causal path from M to \mathbf{Y}_{X_j} under \mathbf{S}_i, X_i . But we also know that by the condition that $X_j \in [X_i]$, $\mathbf{Y}_{X_j} \cap \mathbf{Y}_{X_i}$. This means that there is also an active path from $\tau^{(j)}$ to \mathbf{Y}_{X_i} under \mathbf{S}_i, X_i which clearly contradicts with the fact that $(\tau^{(j)} \perp\!\!\!\perp \mathbf{Y}_{X_i} | X_i, \mathbf{S}_i)$ in \mathcal{G}_π . Thus, $(\tau^{(j)} \perp\!\!\!\perp \mathbf{Y}_{X_i} | [X_i], \mathbf{S}_{[X_i]})$ in \mathcal{G}_π holds. Now, we can view the whole $[X_i]$ as one high-level action and follow a similar induction procedure as in the simpler case, which completes the proof. \square

Proof of Thm. 2 We first show that the maximal editable set w.r.t. a set of actions is unique. Let $K = \max_{\mathbf{V}_I^{(j)}} |\mathbf{V}_I^{(j)}|$. If there are two maximal admissible sets $\mathbf{V}_1, \mathbf{V}_2$ w.r.t $\mathbf{X}^{(j)}$, they satisfy $|\mathbf{V}_1| = |\mathbf{V}_2| = K$ but $\mathbf{V}_1 \neq \mathbf{V}_2$. Interchangeably, we can assume a state variable $V \in \mathbf{V}_1$ but $V \notin \mathbf{V}_2$ exists. Since V satisfies our criterion, so does every variable in \mathbf{V}_2 . Then by Def. 4 we know the set $\mathbf{V}' = \mathbf{V}_2 \cup \{V\}$ is admissible w.r.t $\mathbf{X}^{(j)}$, which contradicts with the fact that \mathbf{V}_2 is the maximal set since $|\mathbf{V}'| = K + 1$. Thus, this is impossible to happen.

By the uniqueness, we only need to search for one maximal editable set w.r.t a given set of actions $\mathbf{X}^{(j)}$. For each variable, by Def. 4 it has to be admissible w.r.t $\mathbf{X}^{(j)}$ before it can be added to the admissible set $\Delta^{(j)}$. Thus, we loop through all state variables and check their editability. If a single state variable is not admissible w.r.t an action, $X \in \mathbf{X}^{(j)}$, we don't need to check its editability w.r.t other actions further. So, we can break the loop there. The editability check is done on the augmented graph \mathcal{G}_π where a pseudo edit indicator τ is added, pointing to V , the state variable being checked. The correctness of this step is guaranteed by the correctness of TESTSEP (van der Zander et al. 2014). \square

Proof of Thm. 3 Since every source task we use is causally aligned, the optimal decision rules of actions in $\mathbf{X}^{(j)}$ will be invariant across the target task and the source task $\mathcal{T}^{(j)}$. The same is true for the set of actions $\mathbf{X}^{(j+1)}$. By our construction, we have $\mathbf{X}^{(j)} \subseteq \mathbf{X}^{(j+1)}$, and each action corresponds to exactly one element in $\pi^{(j)} \cap \pi^*, \pi^{(j+1)} \cap \pi^*$, respectively. Thus, the set of invariant optimal decision rules is also expanding. \square

Proof of Corol. 1 By the correctness of FINDMAXEDIT, we know that every source task generated by $\text{GEN}(\mathcal{T}, \Delta^{(j)})$ will be causally aligned w.r.t $\mathbf{X}^{(j)}$. Then by the way we construct $\mathbf{X}^{(j)}$, it is guaranteed that $\mathbf{X}^{(j)} \subseteq \mathbf{X}^{(j+1)}$. Thus, the returned curriculum of FINDCAUSALCURRICULUM will be causally aligned. \square

Proof of Thm. 4 This is a direct result of applying Lem. 1 to soluble target tasks. \square

Proof of Thm. 5 The algorithm works by creating source tasks with an expanding set of actions. The set of actions expands in the direction that follows the soluble ordering, $\mathbf{X}' = \{X_N, X_{N-1}, \dots, X_1\}$. Then, by Thm. 4 the editable set can be calculated w.r.t only the newly added action in this round (X_i). The while loop ensures we generate enough source tasks to cover all the possible state inputs to X_i . Note that we don't require the final output $\pi^*(\mathcal{C})$ to be optimal in all source tasks. It is still the optimal target task policy. Because given the expanding action sets when constructing source tasks, optimal decision rules of $\mathbf{X}^{(j-1)}$ learned in $T^{(j-1)}$ are still optimal in $T^{(j)}$ and the final output policy $\pi^*(\mathcal{C})$ will contain optimal decision rules for all actions \mathbf{X} in the target task. \square

F EXPERIMENT AND IMPLEMENTATION DETAILS

This section introduces the details of our experiments, including environment specifications, agent hyper-parameters, training/testing protocols, and more experimental results. For the Colored Sokoban and the Button Maze, we implemented a Proximal Policy Optimization (PPO) agent with independent actor and critic networks in PyTorch (Schulman et al., 2017). Both networks have three convolutional layers and two linear layers with rectified linear unit (ReLU) activation functions. The number of output channels of the convolutional layers is [32, 64, 64] with each layer. For convolutional kernels in those three convolutional layers, we use 8×8 with a stride of 4, 4×4 with a stride of 2, and 3×3 with a stride of 1, respectively. We flatten the output of the convolutional layers and feed it into the two linear layers with the intermediate feature dimension set to 512. The input for the network is an image observation of size $84 \times 84 \times 3$ for both environments. For hyper-parameters, we follow the default hyper-parameters from Huang et al. (2022b) on which the implementation is also heavily based. For the Continuous Button Maze environment, we use an Soft Actor Critic (SAC) agent with low-dimensional state vector inputs following the implementations by Huang et al. and adopting the hyper parameters setting from Klink et al. For the four curriculum generators used, we adopted the implementation from Klink et al. (2022)'s official implementations (<https://github.com/psclink/currot>). Note that even though all three environments are confounded, we still use MDP-based policy learning algorithms. Because for those environments, in both target task and aligned source tasks, the confounder is revealed by other variables without intervention. Thus, the agent has perfect information to decide which state it is in exactly. So, we can still use PPO and SAC to find the optimal policy.

F.1 ENVIRONMENT SPECIFICATIONS

For Colored Sokoban, the target task definition is already specified in Example 1

For Button Maze, at each time step, let C_i be the target location's color, B_i be the button status of whether it has been pushed or not, L_i be the agent's current location, Y_i be the reward for this step and X_i be the agent's action in this step. $B_i = \neg B_{i-1}$ when the agent pushes the button. The goal location's color $C_i = U_i$ before the button is pushed but $C_i = U_C$ after the button is pushed, where $P(U_i = 1) = 1/2$, $P(U_C = 1) = 1/5$. The reward function is specified as follows,

$$Y_i = \begin{cases} 1 & \text{if } B_i = \text{"next to goal"} \wedge X_i = \text{"move forward"} \wedge (U_C = 1) \\ -1 & \text{if } B_i = \text{"next to goal"} \wedge X_i = \text{"move forward"} \wedge (U_C = 0) \\ -0.1 & \text{if } L_i = L_{i-1} \\ -0.01 & \text{otherwise} \end{cases}. \quad (29)$$

In the Continuous Button Maze environment Fig. 8 similar to the grid-world button maze, the agent also must navigate to the target region at the right time. The only difference is that this time the environment is an open area and all states and actions are in the continuous domain, which is exponentially large. The optimal strategy for the agent is still to push the button first then step onto the green goal region. Note that the goal region flashes between red and green color before pushing the button. Even if the agent step onto it when it shows green, it is still possible that the agent gets a negative reward. The environment is defined the same as the Button Maze with the only difference

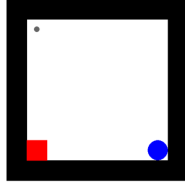


Figure 8: Continuous Button Maze. The agent (the grey dot) needs to navigate the room and step into the goal region (the region in the bottom left) at the right time. The goal region flashes between red and green. And after pushing the button, it will be always green.

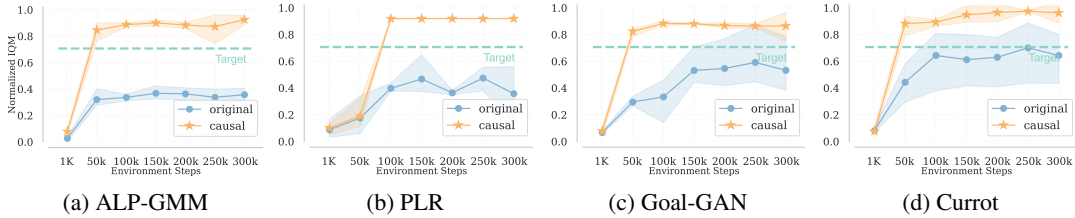


Figure 9: Target task performance of the agents at different training stages in the Continuous Button Maze using different curriculum generators (Columns). The horizontal green line shows the performance of the agent trained directly in the target. “original” refers to the unaugmented curriculum generator and “causal” refers to its causally augmented version.

that we remove the not-moving penalty from the reward function,

$$Y_i = \begin{cases} 1 & \text{if } B_i = \text{“next to goal”} \wedge X_i = \text{“move to the goal”} \wedge (U_C = 1) \\ -1 & \text{if } B_i = \text{“next to goal”} \wedge X_i = \text{“move to the goal”} \wedge (U_C = 0) \\ -0.01 & \text{otherwise} \end{cases} \quad (30)$$

The curriculum generators are allowed to pick the initial location of the agents, whether to toggle the button at the beginning, and whether to intervene the goal region color.

F.2 ADDITIONAL EXPERIMENT RESULTS

When reporting results, instead of using the cumulative rewards directly, as promoted in Agarwal et al. (2021), we report the Interquartile Mean (IQM) normalized by the maximum and minimum rewards in the corresponding environment. Specifically, for each experiment, we run five random seeds. Then, the normalized IQM is calculated as,

$$\text{NORMALIZED IQM} = \frac{2}{n} \sum_{i=\frac{n}{4}+1}^{\frac{3n}{4}} \frac{(x_i - l)}{(u - l)} \quad (31)$$

where x_i are the original data points we collected and sorted, e.g., cumulative rewards, and $\forall x_i, x_i \in [b, u], b, u \in \mathbb{R}$ are the bounds for the data points. In our experiments, the bounds for the rewards are easily obtainable as they are both artificially designed game environments. In the implementation, we edit the environment by editing a set of predefined parameters. Each vector of parameters corresponds to a unique instance of the environment.

In Fig. 9 we see that agent trained by causal agnostic curriculum generators fail to avoid misaligned source tasks and unable to converge to the optimal policy. Those agents trained by the curriculum generators perform even worse than those directly trained in the target task which verifies the necessity of avoiding misaligned source tasks empirically. After augmenting the same curriculum generators with our algorithm, agents trained by them all successfully converge to the optimal surpassing those trained directly in the target task. The result demonstrates that our method is indeed widely applicable to both high-dimensional and continuous domains and that utilizing qualitative causal knowledge properly is crucial to the successful application of curriculum learning in the confounded environments.

Table 2: Misaligned Source Task Portion.

Env./Alg.	ALP-GMM	PLR	Goal-GAN	Currot
Colored Sokoban	68.10 \pm 0.71%	69.10 \pm 2.77%	66.41 \pm 1.84%	68.36 \pm 1.06%
Button Maze	88.41 \pm 0.43%	87.33 \pm 3.77%	90.30 \pm 0.27%	88.62 \pm 1.00%
Con. Button Maze	85.77 \pm 0.83%	83.57 \pm 14.5%	80.55 \pm 19.6%	47.70 \pm 32%

During the training process, we also counted the portions of misaligned source tasks generated by those non-causal curriculum generators. From Table 2 we see clearly that in all three environments, those curriculum generators fail to avoid misaligned source tasks and most of the source tasks proposed by them are actually misaligned. We report those portions with 95% confidence intervals.

We also show examples of the curricula generated by those augmented generators in Figs. 10 to 12

G DETAILED RELATED WORK

Research in generating suitable curricula for reinforcement learning agents can date back to the 90s when people manually designed subtasks for robot controlling problems Sanger (1994). In recent works, a general curriculum generation framework requires two components, an encoded task space and a task characterization function (Narvekar et al. 2020; Wang et al. 2020). Each component may be either hand-coded as inputs (Khan et al. 2011; Peng et al. 2018; MacAlpine & Stone 2018; Portelas et al. 2019) or automatically learned from data along with training the agents (Parker-Holder et al. 2022; Klink et al. 2022; Florensa et al. 2018; Jiang et al. 2021; Florensa et al. 2017; Risi & Togelius 2020; Cho et al. 2023; Huang et al. 2022a). A straightforward task space encoding is to split the observation with common patterns (e.g. pixel tiles) and re-combine them to create new tasks (Dahlskog & Togelius 2014), which can be intractable in the face of a rich observation space and adds extra representational burdens to the curriculum generator. Recent work usually uses vectored parameters as task space encoding, each of which can be grounded into a unique task instance (Parker-Holder et al. 2022; Klink et al. 2022; Florensa et al. 2018; Jiang et al. 2021; Portelas et al. 2019; Dennis et al. 2020; Wang et al. 2019; 2020; Cho et al. 2023; Huang et al. 2022a). While parameter-based encoding is widely applicable in various decision-making tasks, using a dedicated domain description language such as Video Game Description Language (VGDL) for task space encoding provides finer granularity and readability in task generation (Schaul 2013; Liebana et al. 2016; Justesen et al. 2018). A suitable task space encoding then lays the foundation of a reasonable task characterization function, which is either a task difficulty measure (Florensa et al. 2018; Parker-Holder et al. 2022; Dennis et al. 2020; Andreas et al. 2017; Sukhbaatar et al. 2018; Jiang et al. 2021) or a task similarity function (Svetlik et al. 2017; Silva & Costa 2018; Jiang et al. 2021; Eysenbach et al. 2019) in general. For example, task similarity can be measured via domain knowledge based heuristics (Svetlik et al. 2017; Andrychowicz et al. 2017; Silva & Costa 2018) and agent’s performance can be used as a direct indicator of the task difficulty (Florensa et al. 2017; 2018; Narvekar et al. 2017; Parker-Holder et al. 2022). Curriculum generator relies heavily on these task characteristic functions to measure the quality of the task, schedule the training process, and evaluate the agent’s performance (Narvekar et al. 2020; Portelas et al. 2020).

Given task space encoding and task characteristic functions, the remaining central problem of curriculum learning is how exactly one could generate new tasks efficiently. The most intuitive idea of training agents on increasingly harder tasks has been verified in various works, which can be implemented as setting different goals (Florensa et al. 2018; Racanière et al. 2019; Baranes & Oudeyer 2013) or changing starting state distributions (Florensa et al. 2017; Salimans & Chen 2018; Asada et al. 1996; Narvekar et al. 2016). Another major branch of task generation is to change task’s state space or task parameters. This approach usually works together with a parametrized task space where all state factors and transition function parameters are fully encoded as a latent vector (Parker-Holder et al. 2022; Klink et al. 2022; Florensa et al. 2018; Jiang et al. 2021; Portelas et al. 2019; Dennis et al. 2020; Wang et al. 2019; 2020; Cho et al. 2023; Huang et al. 2022a). When more flexibility is desired, source tasks can also be generated by changing the transition or reward function forms. In curiosity-driven agents, exploration is encouraged by an intrinsic reward added upon

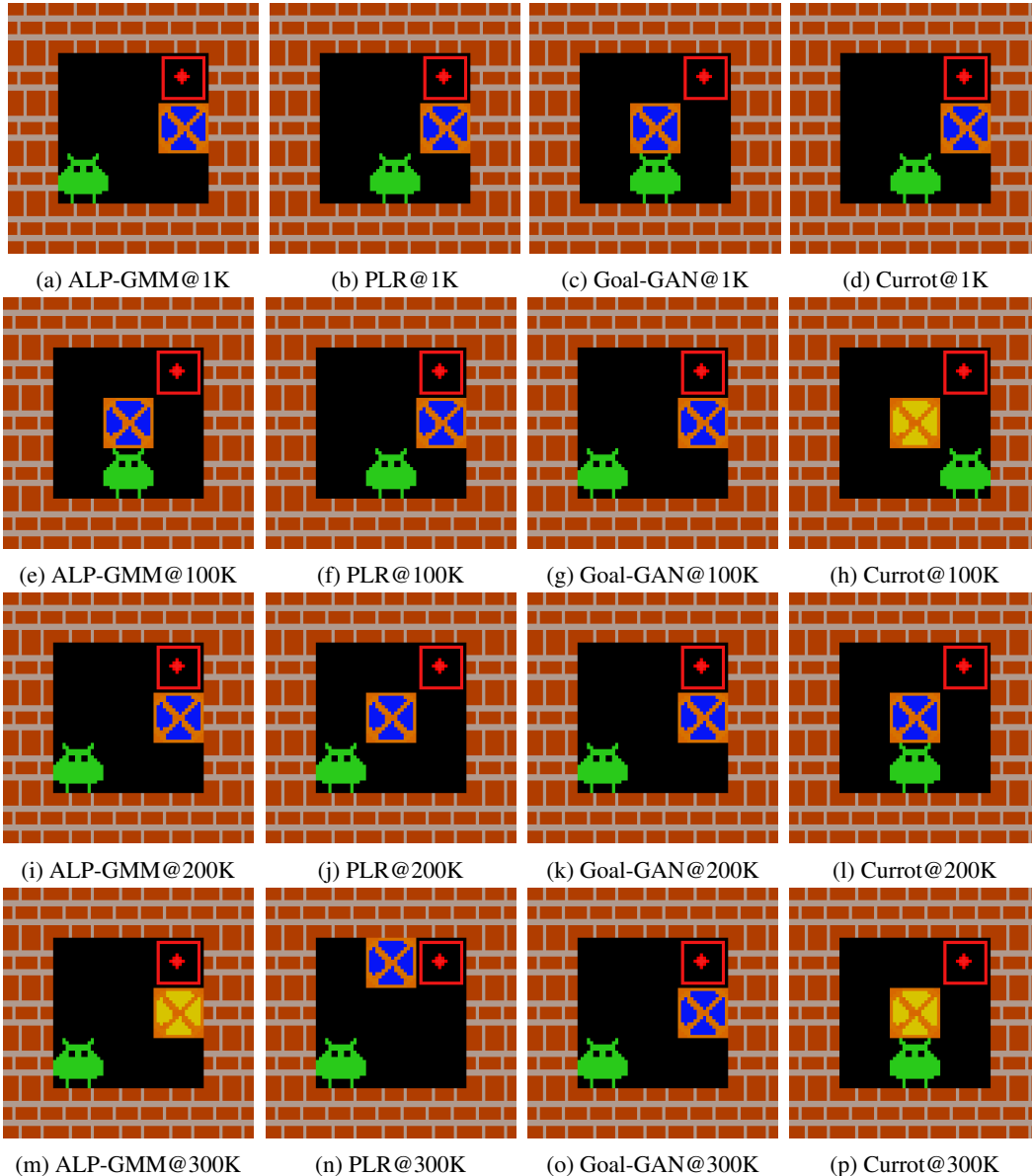


Figure 10: Curricula generated by the (causal) augmented curriculum generators for Colored Sokoban. Each column shows a curriculum from one generator at different training steps.

the original reward from the task (Bellemare et al., 2016; Ecoffet et al., 2019), and this intrinsic reward signal can be learnable which evolves as agents progress in the task (Burda et al., 2019; Singh et al., 2004). Another telling illustration of function forms change is the Sim2Real problem. When generating tasks for a robot in simulation, other than a simulated perfect dynamics model, one needs to take into account extra fractions, inaccurate sensors, motor latency, and poorly executed actions for a successful deployment into the real-world target task (OpenAI et al., 2019).

The crux of curriculum reinforcement learning is to transfer useful knowledge from subtasks to target tasks (Narvekar et al., 2020), which can be modeled as a transportability problem in the causal literature (Correa & Bareinboim, 2020; Pearl & Bareinboim, 2011; Bareinboim & Pearl, 2016). The literature on transportability studies broadly how to answer queries with data from disparate domains. By examining shared causal mechanisms across seemingly dissimilar domains, formal graphical conditions are established to identify what queries can be answered and how those should be answered. In our curriculum reinforcement learning setting, a good curriculum elicits policy

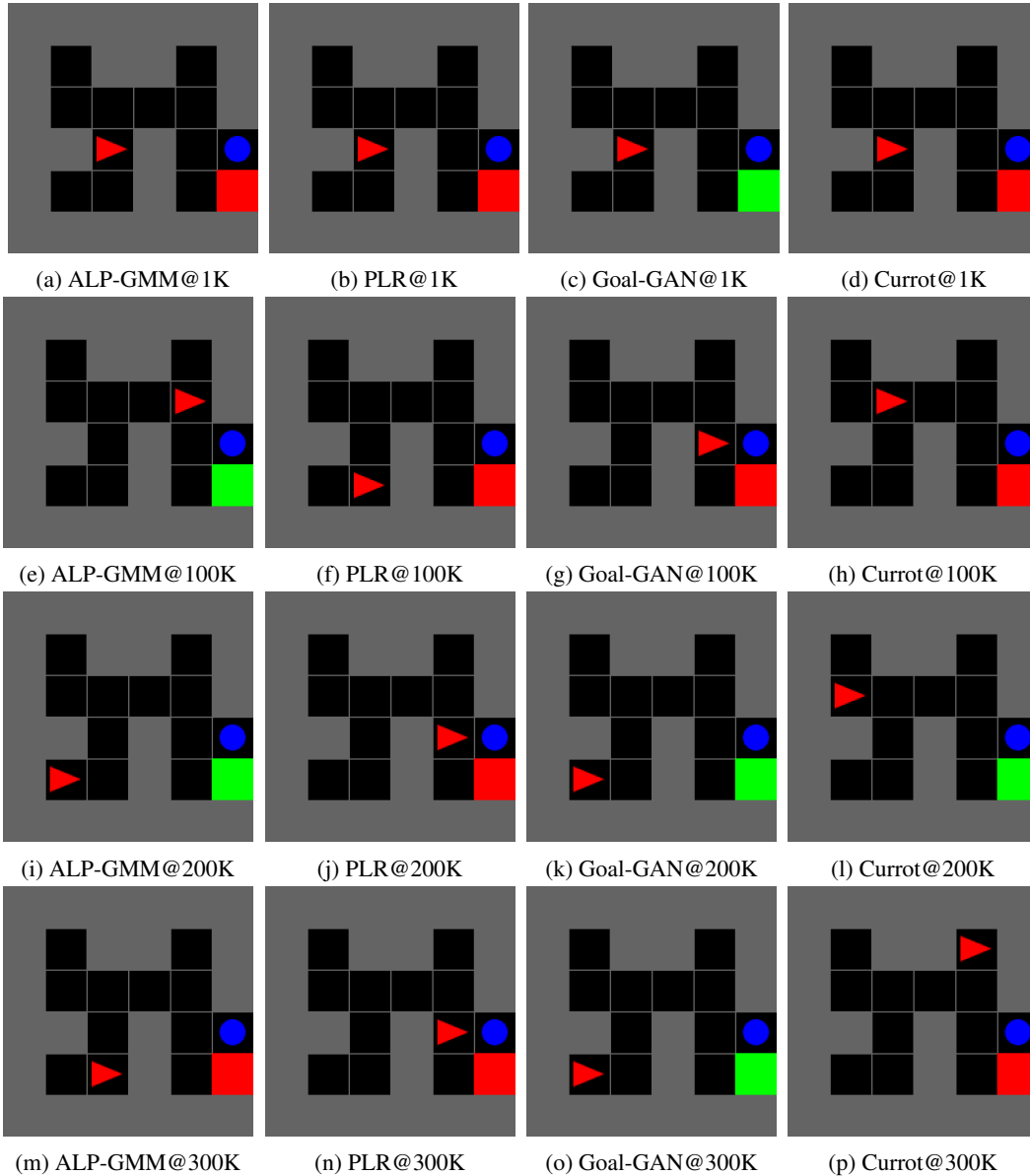


Figure 11: Curricula generated by the (causal) augmented curriculum generators for Button Maze. Each column shows a curriculum from one generator at different training steps.

that performs well not only in subtasks but, more importantly, in target tasks. Policy pieces from various tasks in the curricula constitute our data from which our quest is to construct an optimal target task policy. Since subtasks are generated from target tasks, they share certain aspects in principle. Analyzing how we can transfer those policy pieces to the target tasks can thus be viewed as a transportability problem.

Throughout the paper, we assume access to the causal diagram of the task. However, there is also an orthogonal line of research dedicated in learning the causal structure directly from the task from which a causal diagram can be derived naturally (Hu et al., 2022; Li et al., 2023; Perry et al., 2022).

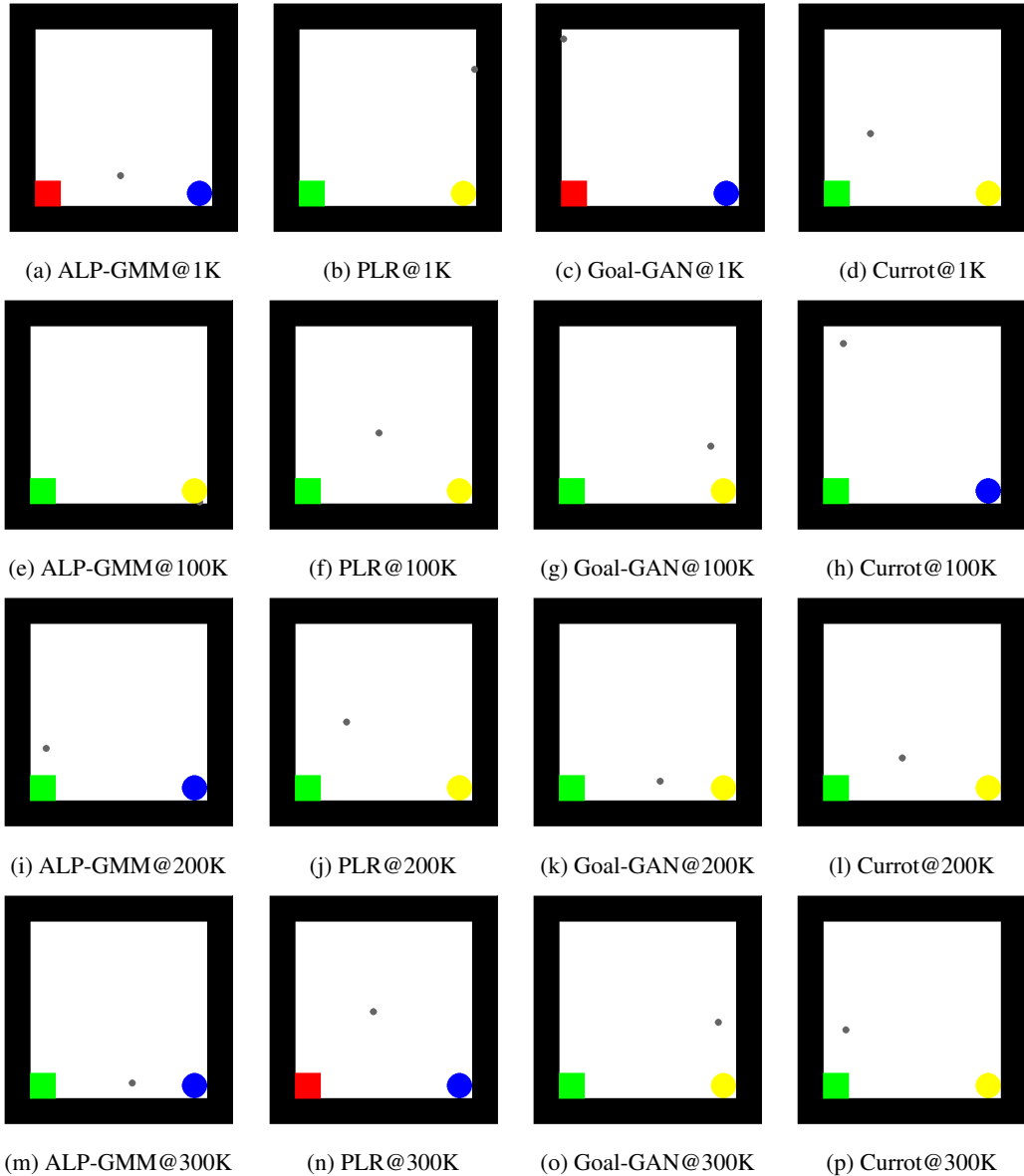


Figure 12: Curricula generated by the (causal) augmented curriculum generators for the Continuous Button Maze. Each column shows a curriculum from one generator at different training steps.

H MARKOV DECISION PROCESSES (MDPs), PARTIALLY OBSERVABLE MDPs (POMDPs), AND STRUCTURAL CAUSAL MODELS (SCMs)

An MDP is defined to be a four-tuple $\langle \mathcal{S}, \mathcal{A}, \mathcal{R}, T \rangle$ where \mathcal{S} is a finite set of states, \mathcal{A} a finite set of actions, $T : \mathcal{S} \times \mathcal{A} \rightarrow \Pi(\mathcal{S})$ the transition function mapping from state action pair to the distribution over the set of states and $\mathcal{R} : \mathcal{S} \times \mathcal{A} \rightarrow \mathbb{R}$ the reward function (Kaelbling et al., 1996). And a POMDP is defined to be a six tuple with two additional elements than the MDP, $\langle \mathcal{S}, \mathcal{A}, \mathcal{R}, T \rangle, \mathcal{O}, p$ where \mathcal{O} is a finite set of observations and $p : \mathcal{S} \rightarrow \Pi(\mathcal{O})$ is the observation function mapping from the true underlying state to the distribution of observations (Kaelbling et al., 1998). Recall the definition of SCMs in the preliminary section, we can see that the definition of SCMs subsumes the transition function and inherent structural assumptions in MDPs and POMDPs. We can encode all the state/action/observation/reward variables as endogenous variables and the randomness of the

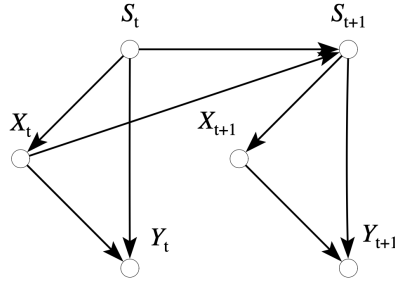


Figure 13: The causal diagram of a standard MDP. We use X to denote actions and Y to denote rewards.

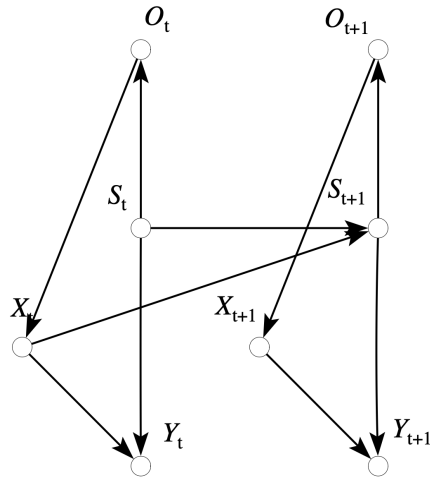


Figure 14: The causal diagram of a standard POMDP. We use X to denote actions and Y to denote rewards.

reward and transition functions as exogenous variables. Each variable's value is either determined by a structural equation specified by the environment or a policy specified by the agent.

Graphically speaking, the causal diagram of a typical MDP is shown in Fig. 13. The next state S_{t+1} only takes the action and state at the current time step as input, which means that in the form of structural equations, $S_{t+1} = f_{S_{t+1}}(S_t, X_t, U_{S_{t+1}})$ where $U_{S_{t+1}}$ is an exogenous variable representing the inherent randomness in the transition function. In Fig. 13, we can see clearly the Markov assumption embedded inside the graphical structure, i.e., $(S_{t+1} \perp\!\!\!\perp S_{t-1} | S_t, X_t)$. Similarly, we can also ground the Markovian reward assumption with precise graphical criteria. As stated by Abel et al., Markovian reward assumption assumes that the state factors that are affecting the reward are fully observable to the agent. This can be interpreted as, $pa(Y_t) \subseteq S_t$ where all parent nodes of the reward node is given as input to the agent (S_t). Note that here we denote the state as a set of variables instead of one single variable for clarity and we implicitly assume that the agent can observe all S_t when making decisions.

For POMDP, the causal diagram is shown in Fig. 14. The causal diagram faithfully reflects the fact that the agent cannot observe the state variables directly but only the observations. And importantly,

the underlying transition dynamics between the true states and actions are still following the standard MDP. The representation of SCMs is more versatile in modeling decision making scenarios in that it is amenable to represent any data generating processes without casting structural assumptions like MDP nor POMDP to the problem. By introducing the notion of confounders, we can better utilize the graphical structure to construct optimal agents efficiently (Zhang & Bareinboim, 2020).

In this work, we utilize the qualitative causal knowledge to ensure that the causal effect of changing certain aspects of the target task won't affect the optimal policy the agent will learn from the generated source task. Even without confounders, if the state space is partially observable, the same situation as in the Colored Sokoban could happen since not all factors affecting the reward can be observed by the agent. But when the Markovian reward assumption holds, where the agent can observe all the parents of the reward variable, the reward cannot be confounded with any other variables. Under this stronger assumption, as our Theorem 1 indicates, all state variables are editable. On the other hand, we are dedicated to solving the curriculum generation problem in the presence of unobserved confounders. Thus, the setting of Markovian rewards actually falls into the traditional curriculum reinforcement learning problem studied in the literature, which our work is trying to relax.